

**This manuscript is a pre-print that has been accepted for publication in Tectonics.**

---



## 24 **Abstract**

25 The northern North Sea rift evolved through multiple rift phases within a highly heterogeneous  
26 crystalline basement. The geometry and evolution of syn-rift depocentres during this multiphase  
27 evolution, and the mechanisms and extent to which they were influenced by pre-existing structural  
28 heterogeneities remain elusive, particularly at the regional scale.

29 Using an extensive database of borehole-constrained 2D seismic reflection data, we examine how the  
30 physiography of the northern North Sea rift evolved throughout late Permian-Early Triassic (RP1) and  
31 Late Jurassic-Early Cretaceous (RP2) rift phases, and assess the influence of basement structures  
32 related to the Caledonian orogeny and subsequent Devonian extension. During RP1, the location of  
33 major depocentres, the Stord and East Shetland basins, was controlled by favorably oriented Devonian  
34 shear zones. RP2 shows a diminished influence from structural heterogeneities, activity localises along  
35 the Viking-Sogn graben system and the East Shetland Basin, with negligible activity in the Stord  
36 Basin and Horda Platform. The Utsira High and the Devonian Lomre Shear Zone form the eastern  
37 barrier to rift activity during RP2. Towards the end of RP2, rift activity migrated northwards as  
38 extension related to opening of the proto-North Atlantic becomes the dominant regional stress as rift  
39 activity in the northern North Sea decreases.

40 Through documenting the evolving syn-rift depocentres of the northern North Sea rift, we show how  
41 structural heterogeneities and prior rift phases influence regional rift physiography and kinematics,  
42 controlling the segmentation of depocentres, as well as the locations, styles and magnitude of fault  
43 activity and reactivation during subsequent events.

44

45

## 46 **1 Introduction**

47 Continental rifts often develop through multiple phases of extension within lithosphere containing  
48 structural heterogeneities inherited from earlier orogenic events. At the regional scale, faults from  
49 prior rift phases and pre-existing structural heterogeneities may be reactivated in some areas during  
50 later rift phases whilst remain inactive in others, resulting in the migration of syn-rift depocentres and  
51 fault activity throughout the evolution of a rift. The evolution of rift systems throughout these multiple  
52 superposed tectonic events records the influence of any pre-existing structural heterogeneities within  
53 the lithosphere.

54 Pre-existing structures, along with early phases of rifting, can exert a considerable influence over the  
55 distribution of fault activity and the geometry and evolution of syn-rift depocentres during subsequent  
56 rift phases. Pervasive basement fabrics can directly control the geometry of faults and the (rift) basins  
57 they bound (e.g. Daly et al., 1989; Fazlikhani et al., 2017; Gontijo-Pascutti et al., 2010; Morley et al.,  
58 2004; Paton and Underhill, 2004; Phillips et al., 2016; Phillips et al., 2017; Salomon et al., 2015;  
59 Skyttä et al., 2019; Vasconcelos et al., 2019). Discrete structures may also locally perturb the regional  
60 stress field, causing faults to strike oblique to the regional extension direction (Corti, 2008; Corti et al.,  
61 2007; Morley, 2010, 2017; Philippon et al., 2015; Rotevatn et al., 2018; Samsu et al., 2019). In other  
62 instances, pre-rift basement structures may also retard lateral fault propagation and thus cause fault  
63 and rift segmentation (Brune et al., 2017; Fossen et al., 2016; Koopmann et al., 2014). Earlier phases  
64 of extension may also modify the crustal and lithospheric structure of rift systems. Faults related to  
65 earlier rift phases interact with, and may exhibit controls over the growth of newly formed normal  
66 faults (e.g. Bell et al., 2014; Claringbould et al., 2017; Deng et al., 2017a; Duffy et al., 2015; Henstra  
67 et al., 2019; Henstra et al., 2015; Morley, 2017; Nixon et al., 2014); whilst, at the whole-rift scale,  
68 lithospheric thinning associated with earlier phases of extension may focus or dissipate strain during  
69 later rift phases (e.g. Boone et al., 2018; Brune et al., 2017; Claringbould et al., 2017; Cowie et al.,

70 2005; Naliboff and Buiter, 2015; Odinsen et al., 2000). Previous studies often focused on local (<10's  
71 of km) scale aspects of the influence of pre-existing structural heterogeneities on rift geometry and  
72 kinematics, with relatively few studies examining the regional, whole-rift (100's of km) scale (Corti,  
73 2009; Daly et al., 1989; Fazlikhani et al., 2017; Morley, 2017). Furthermore, these studies often do not  
74 consider how structural inheritance is able to influence rift physiography along-strike and in 3D, and  
75 how pre-existing structural heterogeneities may influence fault reactivation and therefore control the  
76 location and geometry of syn-rift depocentres throughout multiple rift phases.

77 In this study, we focus on the northern North Sea rift located between the UK and Norway, which  
78 represents a failed rift marginal to the site of eventual North Atlantic breakup (e.g. Coward et al.,  
79 2003; Dore et al., 1997; Kristoffersen, 1978; Roberts et al., 1999). The underlying crystalline  
80 basement of the rift is highly heterogeneous, containing numerous structures formed during the  
81 Caledonian orogeny and a subsequent period of Devonian extension (e.g. Andersen and Jamtveit,  
82 1990; Bird et al., 2014; Færseth et al., 1995; Fazlikhani et al., 2017; Fossen et al., 2016; Lenhart et al.,  
83 2019; McClay et al., 1986; Phillips et al., 2016; Reeve et al., 2013; Scisciani et al., 2019). The  
84 northern North Sea rift formed in response to two main phases of extension, initiating in the late  
85 Permian-Early Triassic (RP1) with a further phase in the Late Jurassic-Early Cretaceous (RP2) (e.g.  
86 Coward et al., 2003; Færseth, 1996; Ziegler, 1992).

87 Due to its long history of hydrocarbon exploration and production, the northern North Sea rift contains  
88 an abundance of geophysical and geological data, including near-complete coverage by 2D and 3D  
89 seismic reflection data and >6000 boreholes. This rich subsurface dataset has illuminated the tectono-  
90 stratigraphic evolution of the North Sea rift (e.g. Evans et al., 2003), although, due to a previous  
91 relative scarcity of well and seismic data at deeper structural levels, a number of key questions  
92 regarding the early stages of rift evolution remain. Well data are typically collected at relatively  
93 shallow (2-3 km), more economic depths, with few wells penetrating deeper areas, particularly in the  
94 hanging walls of major faults. Previously, imaging of basement structures was confined to regional

95 seismic sections, often limited to 2D and at the expense of resolving shallow structure ((BIRPS) and  
96 (ECORS), 1986; Fossen et al., 2014; Gabrielsen et al., 2015; Klemperer and Hobbs, 1991). However,  
97 more recently basement structures have been resolved beneath the northern North Sea rift, particularly  
98 where they are situated at relatively shallow depths on the rift margins (Bird et al., 2014; Fazlikhani et  
99 al., 2017; Lenhart et al., 2019; Patruno et al., 2019; Phillips et al., 2016; Reeve et al., 2013).

100 Using key borehole-constrained stratigraphic horizons and intervening time-thickness maps covering  
101 the entire width of the northern North Sea rift (100,000 km<sup>2</sup>), along with a detailed catalogue of the  
102 various basement structures (Fazlikhani et al., 2017; Fichler et al., 2011; Fossen et al., 2016;  
103 Lundmark et al., 2013), we characterise the structural style and depocentre geometry of the rift system  
104 throughout late Permian-Early Triassic and Late Jurassic-Early Cretaceous rift phases. The relatively  
105 well constrained basement structures beneath the northern North Sea rift (Færseth et al., 1995;  
106 Fazlikhani et al., 2017; Lenhart et al., 2019; Lundmark et al., 2013; Phillips et al., 2016; Reeve et al.,  
107 2013), in combination with the abundance of geophysical data imaging the deeper levels of the rift,  
108 make it the ideal natural laboratory in which to study how pre-existing structures and multiple phases  
109 of rifting influence the geometric and kinematic development of rift systems.

110 This represents a detailed, regional scale study of depocentre geometry and evolution throughout the  
111 multiphase Permian-Cretaceous evolution of the northern North Sea, a type example of a multiphase  
112 rift system influenced by structural inheritance. We relate our regional-scale observations to individual  
113 basin-scale studies in the northern North Sea, incorporating these earlier studies into a wider regional  
114 context, and other regional studies of rift systems elsewhere. By focusing on the detailed rift  
115 physiography and analyzing the evolving depocentre distribution and fault activity across the northern  
116 North Sea rift, we are able to document along-strike changes in rift physiography throughout multiple  
117 rift phases, and to understand how this physiography was influenced by structural inheritance in 3D.  
118 This study showcases the detailed regional evolution of a multiphase rift system and highlights the

119 variable influence of pre-existing structural heterogeneities spatially across the rift during initial and  
120 subsequent phases of rifting.

121

122

## 123 **2 Regional setting and evolution of the North Sea**

124 The northern North Sea rift, as referred to in this study, encompasses a ~250 x 450 km area (~100,000  
125 km<sup>2</sup>) between the East Shetland Platform and the western Norway coastline, and stretching from the  
126 along-strike continuation of the Møre-Trondelag Fault complex in the north to the E-W parallel with  
127 the southern tip of Norway (~58°N) in the south (Figure 1).

128 The crystalline basement beneath the northern North Sea rift is exposed onshore in Norway, the  
129 Shetland Islands and in northern Scotland. The basement initially formed during the Proterozoic  
130 Sveconorwegian orogeny (Roffeis and Corfu, 2013; Slagstad et al., 2013), before being reworked  
131 during the Ordovician-Devonian Caledonian orogeny (Coward, 1990; McKerrow et al., 2000; Milnes  
132 et al., 1997; Roberts, 2003; Wiest et al., 2018). The Scandian phase of the Caledonian orogeny  
133 involved the collision of Baltica and Laurentia and the closure of the Iapetus Ocean (Gee et al., 2008),  
134 with the further collision of Avalonia to the south (McKerrow et al., 2000). Allocthonous nappes,  
135 including continental terranes from Baltica and Laurentia and oceanic terranes from the Iapetus Ocean  
136 (Fossen and Dunlap, 1998; Hossack and Cooper, 1986; Lundmark et al., 2013), were transported ESE  
137 on a décollement composed of mechanically weak Cambrian-Ordovician shales and phyllites, and  
138 emplaced onto the western margin of Baltica (Fossen and Rykkelid, 1992; Milnes et al., 1997).

139 During the Early Devonian, Caledonian thrusting was succeeded by E-W to NW-SE oriented  
140 extension, affecting an area stretching from onshore western Norway in the east to NE Scotland  
141 (Orcaidian Basin) and Greenland in the west (Fossen, 1992, 2010; McClay et al., 1986; Rey et al.,

142 1997; Rotevatn et al., 2018). This extension was initially accommodated by extensional reactivation of  
143 the basal Caledonian thrust zone (Mode I extension of Fossen, 1992), which accounted for around 30  
144 km of extension across southern Norway. Subsequent extension was accommodated by the formation  
145 of km-scale shear zones that offset the entire Caledonian nappe sequence and which extend deep into  
146 the underlying crust (Mode II extension of Fossen, 1992). Devonian shear zones and basins are  
147 identified onshore western Norway (Fossen and Rykkelid, 1992; Milnes et al., 1997; Seranne and  
148 Seguret, 1987; Vetti and Fossen, 2012). These shear zones extend offshore beneath the northern North  
149 Sea rift and, along with additional structures that are not present onshore, are expressed in seismic  
150 reflection data as packages of coherent intra-basement reflectivity (e.g. Bird et al., 2014; Fazlikhani et  
151 al., 2017; Fossen et al., 2016; Lenhart et al., 2019; Phillips et al., 2016).

152 Following Devonian extension, the North Sea experienced further phases of extension and  
153 compression during the Palaeozoic and Mesozoic (Coward et al., 2003; Ziegler, 1992). E-W oriented  
154 extension and associated magmatism occurred across Central Europe and the southern North Sea  
155 during the late Carboniferous-early Permian, mainly affecting the southern part of the study area  
156 (Figure 1) (Pegrum, 1984; Phillips et al., 2017; Wilson et al., 2004). Post-rift thermal subsidence  
157 following late Carboniferous-early Permian extension led to the formation of the North and South  
158 Permian basins, and deposition of the evaporite-dominated Zechstein Supergroup, which influenced  
159 depocentre distribution in the southern section of the study area (Jackson and Stewart, 2017; Stewart et  
160 al., 2007; Stewart and Coward, 1995). The first major rift phase to have affected the northern North  
161 Sea rift initiated in the late Permian and continued into the Early Triassic (here termed Rift Phase 1;  
162 RP1) (Coward, 1995; Coward et al., 2003; Færseth, 1996; Roberts et al., 1995; Ziegler, 1992).  
163 Extension associated with RP1 postdates the deposition of the Upper Permian Zechstein salt in the  
164 south of the area (Jackson and Lewis, 2013; Ziegler, 1992). The regional extension direction during  
165 RP1 is inferred to be E-W, based on the emplacement of N-S striking Permian-Triassic dykes onshore

166 Norway (Fossen and Dunlap, 1999), forming a dominantly N-S oriented rift (Bell et al., 2014;  
167 Coward, 1995; Færseth, 1996; Roberts et al., 1995; Ter Voorde et al., 2000; Ziegler, 1992).

168 A period of relative tectonic quiescence followed RP1 (Coward et al., 2003; Ziegler, 1992), although  
169 some faults remained active during this so-called ‘intra-rift’ period (Claringbould et al., 2017; Deng et  
170 al., 2017a). Early-Middle Jurassic thermal doming in the Central North Sea resulted in the erosion and  
171 removal of large thicknesses of strata across large parts of the North Sea (Davies et al., 1999; Quirie et  
172 al., 2019; Underhill and Partington, 1993). The collapse of this thermal dome in the Middle to Late  
173 Jurassic was followed by a second rift phase (here termed Rift Phase 2; RP2), with activity lasting  
174 until the Early Cretaceous (Coward et al., 2003; Færseth, 1996; Færseth et al., 1997; Underhill and  
175 Partington, 1993; Ziegler, 1992). Rift activity localized onto the ENE-WSW-striking Witch Ground  
176 Graben in the east, the NNW-SSE-striking Central Graben in the south, and the N-S-striking Viking  
177 Graben in the northern North Sea (Coward et al., 2003; Davies et al., 2001; Færseth, 1996; Odinsen et  
178 al., 2000; Roberts et al., 1995; Ter Voorde et al., 2000).

179 The extension direction during RP2 across the northern North Sea is highly debated, with numerous  
180 studies stating that the extension direction was E-W similar to RP1 (Bartholomew et al., 1993; Bell et  
181 al., 2014; Brun and Tron, 1993; Roberts et al., 1990), whereas others suggest that the extension  
182 direction rotated to NW-SE during RP2 (Færseth, 1996; Færseth et al., 1997). During the latter stages  
183 and following RP2, the main area of extension migrated northwards to the Norwegian Sea and the  
184 opening of the proto-North Atlantic Ocean as the Arctic and Atlantic rift systems to the north and west  
185 linked (Roberts et al., 1999; Stewart et al., 1992; Ziegler, 1992). The offshore extension of the Møre-  
186 Trondelag Fault Zone (Figure 1) formed the boundary between the proto-North Atlantic and North Sea  
187 rifts (Dore et al., 1997).

188

### 189 **3 Data and Methods**

## 190 **3.1 Data**

191 This study uses a compilation of 29 2D seismic reflection surveys (~315,000 km total length) from the  
192 northern North Sea rift (see Fazlikhani et al., 2017). These surveys display a range of orientations,  
193 were acquired over a range of time periods (1980-2012), and have different acquisition and processing  
194 parameters (see Table S1 in supplementary material). Seismic line spacing is typically ~3 km (~6 km  
195 across parts of the East Shetland Basin), allowing the correlation of stratigraphic horizons and  
196 basement structures between individual lines. The majority of the sections used in this study are of a  
197 high quality and image down to ~9 s TWT, allowing us to constrain deeper structures and thus the  
198 early rift history. Stratigraphic horizons are tied to a large number of wells, of which 72 penetrate  
199 crystalline basement (see Table S2 in supplementary material) (Fazlikhani et al., 2017). Structural  
200 measurements were converted from the time to the depth domains using the velocity model of  
201 Fazlikhani et al. (2017), with those at deeper levels of the basin converted using interval velocities  
202 from Christiansson et al. (2000). Although parts of these surveys have been interpreted in local studies  
203 (e.g. Claringbould et al., 2017; Deng et al., 2017a; Duffy et al., 2015), this represents one of the first  
204 studies to integrate the available data with observations from these local studies to resolve the regional  
205 multiphase rift evolution of the whole of the northern North Sea.

## 206 **3.2 Seismic interpretation**

207 We map borehole-constrained stratigraphic horizons to describe the present-day rift geometry at  
208 different structural levels. These horizons represent i) the base of the late Permian-Early Triassic rift  
209 sequence (termed “Base RP1”), affected by both RP1 and RP2; ii) the base of the late Middle Jurassic-  
210 Early Cretaceous rift sequence (termed “Base RP2”), showing deformation solely related to RP2 and  
211 later activity; iii) the Base Cretaceous Unconformity (BCU), representing a prominent horizon within  
212 the upper RP2 interval (termed “Near Top-RP2”); and iv) a conservative “Post-rift” horizon  
213 corresponding to the top Cretaceous, unaffected by RP1 and RP2 activity.

214 Due to the large areal extent of these surfaces, and the potentially diachronous nature of rift activity  
215 across the rift, the mapped surfaces often correspond to different lithostratigraphic units in different  
216 areas and sub-basins (Figure 2). The Base RP1 surface typically corresponds to the base of the Triassic  
217 (i.e. base Smith Bank or Teist Formation; Figure 2), or younger strata where the Triassic is not present  
218 (i.e. structural highs or platform areas). One exception is that, where present, the Base RP1 horizon is  
219 represented by the base of the Zechstein Supergroup (Figure 2). Although this represents a Pre-RP1  
220 interval, it forms a regionally prominent reflection and, in contrast to the Top Zechstein horizon (i.e.  
221 the base Triassic), does not include any short-wavelength relief associated with salt mobilization that  
222 would obscure our observations. The Base RP2 surface corresponds to the Middle Jurassic surface  
223 base Hugin and Sandnes formations in the south, and the base Heather Formation elsewhere. The BCU  
224 is typically taken to mark the syn- to post-RP2 transition across the northern North Sea rift, although  
225 some RP2 fault activity postdates this horizon (Bell et al., 2014; Gabrielsen et al., 2001; Kyrkjebø et  
226 al., 2004). In the basin, this typically corresponds to the base Åsgard Formation (Figure 2), although it  
227 often merges with younger unconformities in shallower areas. The mapped Post-rift horizon is defined  
228 by the top Shetland Group across the entire northern North Sea rift (Figure 2).

229 The Base RP1 surface was mapped with moderate to high confidence across the Åsta Graben, Horda  
230 Platform, Stord Basin and East Shetland Basin due to an abundance of well control and its relatively  
231 shallow burial depth. Where it is situated at deeper levels beneath the axis of the northern North Sea  
232 rift, such as in the Viking and Sogn grabens, we are unable to accurately identify the exact reflection  
233 representing the Base RP1 horizon, although we can identify basin-bounding faults that extend  
234 through and offset the interval. Due to this 'corridor of uncertainty' beneath the North Viking and  
235 Sogn grabens, we are often unable to determine the true depth to the Base RP1 horizon, resulting in  
236 lower confidence in our interpretation of the depth and thickness of RP1 depocentres in these areas.  
237 The shallower horizons were mapped with high confidence across the rift.

238 We calculated time-thickness maps between our key stratigraphic surfaces to examine the multiphase  
239 evolution of the complete northern North Sea rift. The time-thickness map between the Base RP1 and  
240 Base RP2 defines syn-rift strata associated with RP1 (Figure 2). This map incorporates the relatively  
241 thin Pre-RP1 Zechstein Supergroup in the south as well as some RP1 post-rift strata (i.e. Late Triassic-  
242 Middle Jurassic) in the upper parts of the interval beneath the Base RP2 surface. Including these  
243 relatively thin packages of pre- and post-RP1 strata in the much thicker RP1 time-thickness map does  
244 not impact our ability to identify the various syn-rift depocentres, particularly as we also use seismic  
245 sections to identify wedge-shaped packages of growth strata that thicken into the hanging walls of  
246 faults to confirm fault activity during each rift phase. The Base RP2 – Near Top-RP2 time-thickness  
247 map includes all Jurassic strata and records the majority of RP2 syn-rift strata. This is referred to as  
248 the “RP2” isochron. The Near Top-RP2 – Post-rift isochron incorporates any Late RP2 syn-rift strata  
249 and a significant post-rift interval that records the migration of activity from the North Sea to proto  
250 North Atlantic opening, and subsequent onset of post-rift thermal subsidence in the northern North  
251 Sea. This is referred to as the Late-syn- to Post-RP2 time thickness map.

252

## 253 **4 Pre-existing structural framework of the northern North Sea**

254 Based on seismic reflection transects and observations from previous studies, we establish the  
255 presence, orientations and geometry of pre-existing structural heterogeneities beneath the northern  
256 North Sea rift (Figure 3, 4), which we later compare to that of syn-rift depocentres during the  
257 evolution of the rift.

258 Crystalline basement is penetrated by numerous wells across the northern North Sea and has been  
259 interpreted in terms of the tectonic units identified onshore in Norway and Scotland (Lenhart et al.,  
260 2019; Lundmark et al., 2013; Riber et al., 2015; Slagstad et al., 2011). Well penetrations across the  
261 Utsira High, a long-lived structural high in the centre of the northern North Sea rift, indicate that, at

262 least in the top few meters penetrated by the wells, crystalline basement is dominantly granitic (e.g.  
263 wells 16/1-15, 16/5-1, 16/6-1; Figure 4) (Lundmark et al., 2013; Riber et al., 2015; Slagstad et al.,  
264 2011). Slagstad et al. (2011) and Lundmark et al. (2013) present U-Pb ages suggesting that the granitic  
265 basement of the Utsira High formed part of a volcanic arc terrane incorporated into the Caledonian  
266 orogeny. This terrane may also be present beneath the East Shetland Basin and East Shetland  
267 Platform, and the Midland Valley Terrane onshore Scotland (Figure 1) (Fichler et al., 2011; Lundmark  
268 et al., 2013).

269 Mylonitic shear zones associated with the Caledonian orogeny and late syn- to post-Caledonian  
270 Devonian extension have been interpreted on seismic reflection data beneath the northern North Sea  
271 rift, where they are characterized by coherent packages of intrabasement reflectivity (Fazlikhani et al.,  
272 2017; Fossen and Hurich, 2005; Hurich and Kristoffersen, 1988; Phillips et al., 2016; Reeve et al.,  
273 2013). Here we briefly outline the general geometries of those shear zones referred to throughout this  
274 study (for a more detailed description of the shear zones, see Fazlikhani et al., 2017). In the northern  
275 part of the study area, the E-dipping Tampen Shear Zone strikes N-S beneath the eastern margin of the  
276 East Shetland Basin. Further west, the N-S to NE-SW-striking Ninian and Brent shear zones splay  
277 southwards away from the Tampen Shear Zone (Figure 3a, 4) (Fazlikhani et al., 2017). Along the  
278 eastern rift margin, W-plunging corrugations associated with the offshore Nordfjord-Sogn Detachment  
279 increase in dip towards the Sogn Graben (Lenhart et al., 2019) (Figure 4). Some of these corrugations  
280 appear spatially and perhaps kinematically linked with the E-W to NE-SW-striking Lomre Shear Zone  
281 (Figure 4) (Fazlikhani et al., 2017). The NE-SW-striking Hardangerfjord Shear Zone and the N-S-  
282 striking Øygarden Shear Zone lie in the footwall of the Øygarden Fault, with the Hardangerfjord Shear  
283 Zone also situated south of and in the footwall of the Øygarden Shear Zone (Figure 3b, 4). (Fazlikhani  
284 et al., 2017). Further south, the N-S- to NE-SW-striking Karmøy and Stavanger shear zones occur in  
285 the footwall of the Åsta Fault and beneath the Stavanger Platform respectively (Figures 3c, 4) (Bøe et  
286 al., 2010; Phillips et al., 2016; Thon, 1980). The E-dipping Utsira Shear Zone tracks the western

287 margin of the Stord Basin (Figure 3b, 4) (Fazlikhani et al., 2017; Fossen et al., 2016), and is  
288 represented by a series of shallowly E-dipping to sub-horizontal splays beneath the Utsira High  
289 (Figure 3c).

290 Reflections that may be related to the presence of deeply buried sediments can be identified beneath  
291 the Base RP1 surface (Figure 3). Coherent reflectivity beneath the Base RP1 surface across the Horda  
292 Platform may be related to Caledonian basement allochthons, as drilled by well 31/6-1 (Fossen et al.,  
293 2016), or in some areas may represent sedimentary strata (Figure 3a, 4). Further coherent reflectivity  
294 beneath the Base RP1 surface is identified beneath the East Shetland Platform which, based on well  
295 information, is interpreted as Devonian sedimentary strata (Figure 3b) (Patruno and Reid, 2016;  
296 Patruno et al., 2019). Reflectivity beneath the Base RP1 surface in the Ling Depression is interpreted  
297 to correspond to sediments deposited during late Carboniferous-Permian extension, which affected  
298 only the southern margin of the study area, although some Devonian strata may also be present locally  
299 (Heeremans and Faleide, 2004; Heeremans et al., 2004; Jackson and Lewis, 2016; Neumann et al.,  
300 2004).

301

## 302 **5 Present-day physiography of the northern North Sea rift**

303 The Base RP1 surface records the cumulative effects of RP1 and RP2 basement-involved fault activity  
304 and defines a ~200 km wide, predominately N-S oriented rift, bordered by the East Shetland Platform  
305 to the west and the Norwegian mainland to the east (Figure 4). The western margin to the rift is here  
306 termed the Western Boundary Fault (Figures 3, 4), whereas the Øygarden and Åsta faults form the  
307 eastern rift margin south of the Måløy Slope (Figure 3c, 4). No rift-bounding fault is present across the  
308 Måløy Slope itself (Figure 4). The N-S- to NNE-SSW-striking Viking and Sogn grabens define the  
309 axis of the basin, with the Viking Graben comprising three segments, the South, Central and North  
310 (Figure 4).

311 In the northwest of the study area, the ~80 km wide East Shetland Basin contains numerous N-S- to  
312 NE-SW-striking, E- to SE-dipping normal faults. The depth to the Base RP1 surface in the East  
313 Shetland Basin ranges from 3-5 s TWT (~4-7 km) (Figure 3a, 4). To the north, the Base RP1 surface  
314 deepens to 6-7 s TWT (~11 km) across the NE-SW-striking Marulk and Magnus basins (Figure 4).  
315 East of the East Shetland Basin, the NNE-SSW-striking North Viking Graben reaches a depth of 6 s  
316 TWT (~9 km) along its western margin, and to the northeast, the N-S striking Sogn Graben reaches ~8  
317 s TWT (~12 km) and may deepen further to the north (Figure 4). East of the North Viking and Sogn  
318 grabens, the Måløy Slope is characterized by relatively minor (~100 ms TWT (~200 m) throw) W- and  
319 E-dipping faults (Figure 4) (Færseth et al., 1995; Lenhart et al., 2019; Reeve et al., 2015).

320 The Horda Platform is located along the eastern margin of the northern North Sea rift, south of the  
321 Måløy Slope and Lomre Shear Zone and north of the Åsta Graben (Figure 4). This area encompasses  
322 the Stord Basin in the south and the Northern Horda Platform in the north. Its western margin is  
323 formed by the Oseberg Fault Block in the north and the Utsira High further south. The Brage Horst  
324 forms a N-S-striking high to the east of the Oseberg Fault Block (Figure 4). The Northern Horda  
325 Platform is dominated by the N-S-striking, W-dipping Tusse, Vette and Øygarden faults (Figure 4).  
326 Each of these faults displace the Base RP1 surface by ~1 s TWT (~1.5 km) (Duffy et al., 2015; Whipp  
327 et al., 2014) (Figure 3a). The depth to the Base RP1 surface across the Northern Horda Platform  
328 ranges from 3-4 s TWT (~4-7 km). The Vette Fault takes a prominent bend midway along its length  
329 where it strikes E-W and dips to the north. This area corresponds to a 'domain boundary' of Fossen et  
330 al. (2016) that correlates with the subcrop of the Lomre Shear Zone (Figure 4) (Fazlikhani et al.,  
331 2017).

332 The Utsira High represents a major intra-basin high where the Base RP1 surface is at ~1.8 s TWT (~3  
333 km) depth. Northeast-dipping faults define the intra-high Augvald Graben (Olsen et al., 2017). East-  
334 dipping faults separate the Utsira High from the Stord Basin to the east (Figure 4), which, apart from  
335 the W-dipping Øygarden Fault along its eastern margin, is dominated by E-dipping faults (Figure 3b).

336 The Øygarden Fault strikes N-S in the north, changing to NE-SW at the southern end of the Stord  
337 Basin. The E-dipping fault along the western margin of the Stord Basin margin generally strikes N-S,  
338 but changes to strike NE-SW in the north (Figure 4).

339 In the N-S- to NNE-SSW-striking Central segment of the Viking Graben, the Base RP1 surface  
340 reaches a maximum depth of ~7 s TWT (~11 km) and in the Southern segment of the Viking Graben it  
341 reaches depths of ~4 s TWT (~6 km). Along the eastern margin of the Viking Graben, the Beryl  
342 Embayment separates the Southern and Central segments (Figure 4).

343 In the southeast of the study area, the NE-SW-striking Ling Depression separates the Utsira and Sele  
344 highs. Further east, the Åsta Fault is separated from the Øygarden Fault by a ~60 km wide relay ramp  
345 (Figure 4). Zechstein Supergroup evaporites are also present across the south of the study area,  
346 thinning northwards in the South Viking and Åsta grabens, and thickening into the Ling Depression  
347 and Norwegian-Danish Basin. Halite-poor, and largely immobile parts of the evaporite sequence are  
348 present across the Utsira High, whereas a relatively thicker and halite-rich, and thus more mobile salt  
349 is present across the Sele High (Figure 3c) (Olsen et al., 2017; Sorento et al., 2018).

350 The present-day rift physiography at the Base RP2 and shallower depths differs to that of the Base  
351 RP1 surface. The physiography of the Near Top-RP2 (BCU) surface largely mirrors that of Base RP2,  
352 albeit at shallower depths. The rift displays an overall deepening to the north, with the Viking and  
353 Sogn grabens forming the dominant structural elements, and the Marulk and Magnus basins also  
354 representing prominent features (Figure 5a, b). Faults are expressed across the Northern Horda  
355 Platform (Figure 3a), but there are notably few faults expressed in the Stord Basin, which forms a ~80  
356 km wide depression, and the Utsira High (Figure 3b, 5a, b). The South Viking Graben forms a narrow  
357 (~40 km wide) rift which begins to widen northwards along the western margin of the Oseberg Fault  
358 Block (Figure 5). Further north, Base RP2 and Near Top-RP2 surfaces describes a single wide rift  
359 from the East Shetland Basin to the Northern Horda Platform and Måløy Slope (Figure 5).

360 There is very little expression of faulting present across the Post-rift surface (Figure 3, 5c), with only  
361 the rift-bounding Western Boundary Fault expressed at this level. As at the Base RP2 and Near Top-  
362 RP2 surfaces, the rift forms a narrow depression (~55-60 km wide) across the South Viking Graben,  
363 which widens northwards to ~200 km across the East Shetland Basin and Måløy Slope (Figure 5c). In  
364 contrast to underlying surfaces, the deepest point of this surface (~2.6 s TWT; ~3 km) is located above  
365 the South Viking Graben rather than in the north (Figure 5c).

366

## 367 **6 Rift Phase 1 - Late Permian-Early Triassic**

368 Rift Phase 1 depocentres predominantly trend N-S to NE-SW, are located within the hanging walls of  
369 N-S- to NE-SW-striking normal faults and are widely distributed across the northern North Sea rift  
370 (Figure 6). The width of the rift during RP1 is relatively uniform from north to south, with fault  
371 activity distributed across a 170 km wide zone from the East Shetland Basin to Northern Horda  
372 Platform in the north, and a 190 km wide zone from the South Viking Graben to the Åsta Graben in  
373 the south. However, in the south, fault activity is localised in the South Viking Graben and Stord Basin  
374 rift segments, separated by the relatively unfaulted Utsira High (Figure 6). RP1 strata are notably thin  
375 atop the Utsira High, although a ~250 ms (~400 m) thick interval is preserved within the NW-SE-  
376 striking Augvald Graben. A condensed succession of RP1 strata (100-400 ms TWT; 200-600 m)  
377 occurs across the Sele High. No RP1-related strata are preserved on platform areas outside of the main  
378 rift (Figure 6).

379 The main depocentres during RP1 were located in the Stord Basin and Northern Horda Platform along  
380 the eastern side of the rift (Figure 6, 7, 8), and the East Shetland Basin in the west (Figure 6, 9), each  
381 containing up to 3200 ms TWT (~4 km) of RP1 strata. Several internal depocentres were present in the  
382 Stord Basin, the largest of which, located within the hanging wall of the E-dipping fault along the  
383 western basin margin, which strikes N-S in the south and swings to trend NE-SW further north,

384 paralleling the strike of the Utsira Shear Zone (Figure 6). In cross-section, the E-dipping faults within  
385 the Stord Basin appear to root downwards into the Utsira Shear zone (Figure 7). In a similar manner,  
386 the W-dipping Øygarden fault along the eastern margin of the Stord Basin soles onto the underlying  
387 Øygarden and Hardangerfjord shear zones (Figure 4, 7). A half-graben in the hanging wall of the  
388 Øygarden Fault displays clear syn-rift divergent wedges, confirming activity at this time (Figure 7).  
389 This N-S-striking depocentre (2000-2500 ms TWT; ~5 km thick) swings to strike NNE-SSW to the  
390 south where the fault strikes parallel to the Hardangerfjord Shear Zone (Figure 6, 7). To the southwest,  
391 along-strike of the Hardangerfjord Shear Zone, RP1 strata thicken into the bounding faults of the Ling  
392 Depression, which forms a NE-SW-striking graben depocentre containing 800 ms TWT (~1.4 km) of  
393 RP1 strata (Figure 3c). To the east, the Åsta Graben also represents an RP1 depocentre containing  
394 ~700 ms TWT (~1.2 km) thick of RP1 strata (Figure 6).

395 North of the Stord Basin, a N-S-striking depocentre (up to ~2500 ms TWT; ~5 km thick) occurs in the  
396 hanging wall of an E-dipping fault southwest of the Vette Fault (Figure 6). Across the Northern Horda  
397 Platform, the Tusse, Vette and Øygarden faults form N-S-striking half graben depocentres containing  
398 divergent syn-rift wedges (Figure 6, 8). Further north, no RP1 strata are preserved on the Måløy Slope  
399 (Figure 6).

400 On the northeast side of the rift, the East Shetland Basin contains multiple depocentres (up to ~2500  
401 ms TWT; ~5 km thick) in the hanging walls of E-dipping faults (e.g. the Tern, Ninian and Brent  
402 faults), as well as the W-dipping Eider Fault (Figure 3a, 9). The geometry of these depocentres  
403 parallels the underlying Ninian, Brent and Tampen Spur shear zones, and the border faults to these  
404 depocentres also appear to merge together at depth, potentially linking with the underlying shear zones  
405 (Figures 6, 9) (Fazlikhani et al., 2017). North of the East Shetland Basin, the Marulk and Magnus  
406 Basins represent NE-SW-striking depocentres containing up to 2000 ms TWT (~5 km) of RP1 strata.

407 South of the East Shetland Basin, the Central and South Viking graben segments contain ~2000 ms  
408 TWT (~5 km) and ~1500 ms TWT (~3 km) of RP1 strata respectively. Rift Phase 1 activity appears  
409 subdued across the North Viking and Sogn Grabens (Figure 6). However, as we are unable to resolve  
410 the Base RP1 surface accurately in the data used in these areas, the magnitude of the RP1 depocentres  
411 is uncertain and our interpretation represents a minimum estimate of RP1 thickness (Figure 6). As a  
412 result, we cannot be certain that the observed depocentre beneath the Northern Horda Platform does  
413 not extend westwards and merge with that of the East Shetland Basin (Figure 6, 9). Observations from  
414 the East Shetland Basin suggest a regional thickening of Triassic strata towards the east, perhaps  
415 indicating that the depocentres may well merge beneath the North Viking Graben.

416

## 417 **7 Rift Phase 2 – Late Jurassic-Early Cretaceous**

418 The time-thickness map calculated for RP2, between the Base RP2 and Near Top RP2 surfaces,  
419 records the majority of syn-rift activity associated with Late Jurassic-Early Cretaceous rifting (Figure  
420 3, 10). The distribution of fault activity during RP2 differed to that of RP1 (Figure 10). The most  
421 notable feature of the RP2 time-thickness map is that fault activity is focused along the Viking and  
422 Sogn grabens (Figure 10) and not in the Stord Basin and Northern Horda Platform (Figure 6). Rift  
423 activity in the south is localised along the ~25 km wide South Viking Graben, between the East  
424 Shetland Platform in the west and the Utsira High to the east (Figure 7). No RP2 activity is evident in  
425 the Stord Basin (Figure 7, 10). Rift activity widens northwards, with faults active across the Oseberg  
426 Fault Block and Brage Horst (Figure 10) (Færseth and Ravnås, 1998). Further north, a ~700 ms TWT  
427 (~1.2 km) depocentre occurs in the hanging wall of the bend in the Vette Fault. In the north of the  
428 study area, fault activity was distributed over roughly the same area as in RP1 (~190 km), with activity  
429 widening in the east onto the Måløy Slope (Figures 3a, 10). The eastern boundary to the active rift

430 during RP2 appears to follow the Utsira High in the south and the Lomre Shear Zone further north,  
431 with no activity observed east of this boundary (Figure 10).

432 The Viking Graben forms the main depocentre during RP2; individual depocentres, including the  
433 South, Central and Northern segments and the Sogn Graben, contain syn-rift divergent wedges, strike  
434 N-S and have a right stepping relationship to one another (Figure 3, 5). RP2 thicknesses reach 1350  
435 ms TWT (~2.5 km) in the South Viking Graben and 1000 ms TWT (~2 km) in the Central Viking  
436 Graben, increasing to ~1800 ms TWT (~3.2 km) in the Sogn Graben (Figure 10). In the north, the NE-  
437 SW-striking Magnus Basin was a major depocentre during RP2, containing ~700 ms TWT (~1.2 km)  
438 of strata. RP1 faults within the East Shetland Basin were also reactivated during RP2. The Tern, Eider,  
439 Osprey, Brent and Murchison faults each contain RP2 syn-rift divergent wedges (up to ~500 ms TWT;  
440 ~1 km thick) in their hanging walls (Figures 3a, 9) (Claringbould et al., 2017). The thickness of RP2  
441 strata is reduced in certain areas of the East Shetland Basin, particularly in the immediate footwalls of  
442 faults, where RP2 strata are often absent due to erosion by the BCU (Figure 9).

443 Rift Phase 2 strata are mostly isopachous across the Northern Horda Platform (~400 ms TWT; 750 m  
444 thick) with no syn-rift divergent wedges observed in the hanging walls of the Tusse, Vette and  
445 Øygarden Faults (Figure 8, 10). To the west, faults across the Oseberg Fault Block and along the  
446 eastern margin of the Brage Horst were active during RP2, with depocentres containing thicknesses of  
447 up to 500 ms TWT (~1 km) (Figure 3a, 10) (Færseth and Ravnås, 1998). The ~800 ms TWT (~1.5 km)  
448 sedimentary thicknesses in the Stord Basin and Northern Horda Platform have a broad lobate platform  
449 geometry. The presence of clinof orm sequences within these lobate intervals suggests that the lobate  
450 area represents the progradation of the Hardangerfjord and Sognefjord deltaic systems into  
451 accommodation not generated through fault-controlled subsidence (Figure 3b, 7, 10) (Dreyer et al.,  
452 2005; Ravnås and Bondevik, 1997; Ravnås et al., 2000; Sømme et al., 2013). South of the  
453 Hardangerfjord Delta, although a thickness change of ~200 ms TWT (~300 m) occurs across the Åsta  
454 Fault, no growth strata are present in the hanging wall, indicating a lack of tectonic activity on the

455 Åsta Fault at this time (Figure 3c, 10). As with RP1, RP2 strata are thin across most of the Utsira  
456 High.

457

## 458 **8 Late-syn-rift- to Post- Rift Phase 2 – Cretaceous**

459 The late-syn-rift to post- RP2 time-thickness map (termed Late-syn- to Post-RP2), calculated between  
460 the BCU and the Post-rift surface, encompasses the entire Cretaceous interval and largely comprises a  
461 thick post-RP2 succession, although some relatively thin intervals of late RP2 syn-rift strata are  
462 present locally (Figure 9). A large, relatively isopachous unit typically forms the upper part of the  
463 Cretaceous interval, for example, across the East Shetland Basin and Sogn Graben (Figures 9, 12),  
464 indicating widespread thermal subsidence in these areas post-RP2. Divergent stratal wedges are  
465 identified locally in the lower parts of the interval, indicating some syn-rift activity at this time (Figure  
466 8, 9).

467 The distribution of depocentres across the Late-syn- to Post-RP2 time-thickness map is broadly similar  
468 to that recorded during RP2 (i.e. Base RP2 to Near Top-RP2) (Figure 11). The overall thickness of  
469 Late-syn- to Post-RP2 strata increases northwards, from ~950 ms TWT (~1.6 km) in the South Viking  
470 Graben to >3 s TWT (>5 km) in the Marulk and Magnus basins and the Sogn Graben (Figure 11).  
471 Late-syn- to Post-RP2 strata thin towards the south (<500 ms TWT; <800 m), with a thin interval  
472 present in the Stord Basin (Figure 7). The base of individual depocentres appear flatter than those  
473 identified in RP1 and RP2 and internally, the stratigraphy displays less pronounced thickening towards  
474 bounding faults (Figure 11). This indicates a lack of fault activity at this time and a predominance of  
475 post-rift thermal subsidence with, in some cases, the passive infilling of remnant relief related to  
476 earlier phases of rifting (Prosser, 1993).

477 In the south, the South Viking Graben depocentre is bound to the east by the Utsira High, where Late-  
478 syn- to Post-RP2 strata are thin and locally absent (typically <150 ms TWT; <200 m) (Figures 10, 11).  
479 As in RP2, east of the Utsira High, no Late-syn- to Post-RP2 activity is recorded across the Stord  
480 Basin and Åsta Graben. Nevertheless, these areas contain 700-900 ms TWT (~1.2 km) of Late-syn- to  
481 Post-RP2 strata, likely deposited in accommodation related to post-RP1 thermal subsidence, as no RP2  
482 activity occurred in this area (Figure 11). However, on the Northern Horda Platform, Late-syn- to  
483 Post-RP2 depocentres in the hanging walls of the Tusse, Vette and Øygarden Faults contain up to  
484 ~600 ms TWT (~1 km) of Late-syn- to Post-RP2 strata. The majority of this strata forms divergent  
485 wedges (Figures 8, 11), indicating late-to-post RP2 reactivation of these faults (Bell et al., 2014). Late-  
486 syn- to Post-RP2 strata in the hanging wall of the Øygarden Fault are truncated by the overlying Base  
487 Cenozoic unconformity (equivalent to the Top Cretaceous) and therefore do not record the true  
488 depositional thickness (Figure 8).

489 Depocentres in the East Shetland Basin strike N-S in the south, swinging round to NE-SW further  
490 north (Figure 11). These depocentres contain 900-1300 ms TWT (1.6-2.3 km) of Late-syn- to Post-  
491 RP2 strata. These depocentres show limited thickening into the hanging wall of faults (with the  
492 Murchison Fault being an exception; Figure 9) and are typically characterized by sub-horizontal  
493 Cretaceous strata that onlap onto rotated Jurassic strata (Figure 9, 10), indicating a relative lack of  
494 fault activity in the East Shetland Basin at this time. We propose that these depocentres record passive  
495 filling of accommodation generated through Late Jurassic RP2 fault activity.

496 East of the East Shetland Basin, the Sogn Graben forms a large Late-syn- to Post-RP2 depocentre,  
497 containing over 3 s TWT (~5 km) of Cretaceous strata (Figure 11, 12). Syn-rift divergent wedges in  
498 the hanging wall of the eastern border fault of the Sogn Graben indicate that this structure was active  
499 during RP2 and the early stages of Late- Post RP2 (Figure 12). Faults along the western side of the  
500 Sogn Graben were active during RP2, but became inactive with their hanging walls being passively  
501 filled during Late-syn- to Post-RP2. (Figure 12).

502 The generation of the accommodation for the upper post-rift strata in the Late-syn- to Post-RP2  
503 interval appears to be related to thermal subsidence following RP2 activity (Figure 11), as evidenced  
504 by the large thicknesses present in the South and Central Viking grabens (Figure 3b, c). The thickness  
505 of Late-syn- to Post-RP2 strata is locally accentuated by fault activity in the Sogn Graben and Marulk  
506 and Magnus Basins, and local westerly tilting in the north of the study area (Figures 11, 12) (Brekke  
507 and Riis, 1987). The increased thickness of Late-syn- to Post-RP2 strata in the north of the study area  
508 reflects a relative increase in activity related to proto-North Atlantic opening in the Møre Basin –  
509 Faroe-Shetland Basin – Rockall Trough axis to the north of the study area (Kristoffersen, 1978;  
510 Roberts et al., 1999), which is related to a decrease in rift activity in the northern North Sea. The NE-  
511 SW-striking Marulk and Magnus Basins are aligned with the Atlantic rifts and Møre-Trondelag Fault  
512 Complex, reflecting this northwards migration of activity (Figure 11, 13) (Dore et al., 1997;  
513 Gabrielsen et al., 2001).

514

## 515 **9 Discussion**

516 We have explored the kinematic and geometric evolution of the northern North Sea rift throughout late  
517 Permian-Early Triassic (RP1) and Late Jurassic-Early Cretaceous (RP2) rift phases (Figure 13).

518 Drawing on these observations, and those from other rift systems worldwide, we first discuss how pre-  
519 existing structures influence the initial rift physiography, before examining how the rift physiography  
520 and kinematics evolves during multiple phases of rifting.

### 521 **9.1 Reactivation and inheritance of basement shear zones during** 522 **rifting**

523 Basement shear zones display a range of strikes beneath the northern North Sea rift (Figure 4).  
524 Numerical modelling, along with previous studies from the North Sea show that shear zones that strike  
525 within 45-90° of the regional extension direction, i.e. close to perpendicular, and have dips greater  
526 than 30° are able to influence fault strike during rifting. Rift-related faults often align in map view  
527 with shear zones displaying these characteristics (Bird et al., 2014; Deng et al., 2017b; Fazlikhani et  
528 al., 2017; Phillips et al., 2016). In the northern North Sea, the Åsta Fault strikes parallel to the offshore  
529 continuation of the Karmøy Shear Zone, whilst the Ling Depression parallels the offshore continuation  
530 of the Hardangerfjord Shear Zone (Fazlikhani et al., 2017; Fossen and Hurich, 2005; Phillips et al.,  
531 2016). Similarly, the dominant N-S to NE-SW strike of faults in the East Shetland Basin parallels the  
532 underlying N-S- to NE-SW-striking Tampen, Brent and Ninian shear zones (Figure 4, 6, 13).  
533 However, in areas such as the Måløy Slope, shear zones strike sub-parallel to the interpreted E-W  
534 oriented regional stress field and are therefore oriented at high angles to rift-related faults, bearing  
535 little influence over their strike (Figure 13).

536 There are multiple geometric and kinematic interactions between basement shear zones and rift-related  
537 faults. Rift-related faults have previously been shown to exploit internal mylonitic layers within shear  
538 zones (Gontijo-Pascutti et al., 2010; Heilman et al., 2019; Kirkpatrick et al., 2013; Morley, 2017;  
539 Paton and Underhill, 2004; Salomon et al., 2015), with examples also documented from the northern  
540 North Sea rift (Figure 15) ('explosive' interaction of Fazlikhani et al., 2017; Phillips et al., 2016).  
541 Numerical and analog modelling has shown that rocks containing a fabric are weaker, and thus more  
542 likely to fail, along said fabric when subject to favorably oriented stress fields (Chattopadhyay and  
543 Chakra, 2013; Tong and Yin, 2011; Youash, 1969; Zang and Stephansson, 2009).

544 Basement shear zones in the northern North Sea may also locally perturb the regional stress field,  
545 causing nearby or newly-formed faults to locally align with the pre-existing structure rather than  
546 perpendicular to the extension direction ('merging' interaction of Phillips et al., 2016) (Figure 15). In  
547 the northern North Sea, the southern extension of the otherwise N-S-striking Øygarden Fault rotates to

548 a NE-SW orientation and locally aligns with the NE-SW-striking Hardangerfjord Shear Zone,  
549 suggesting a local NE-SW-oriented stress field associated with the shear zone (Figure 6, 15). The  
550 Hardangerfjord shear zone represents a major structure across the northern North Sea rift and is  
551 associated with a Moho offset at depth (Gabrielsen et al., 2015; Maystrenko et al., 2017). Similarly,  
552 faults defining the western margin of the Stord Basin follow the underlying Utsira Shear Zone in plan-  
553 view, rotating from N-S in the south to NE-SW further north. These faults merging with the shear  
554 zone at depth (Fazlikhani et al., 2017) (Figure 7). Instances where pre-existing heterogeneities locally  
555 perturbed the regional stress field have also been interpreted in the East African Rift (Corti et al.,  
556 2007; Philippon et al., 2015), the Gippsland Basin offshore Australia (Samsu et al., 2019), the  
557 Taranaki Basin offshore New Zealand (Collanega et al., 2018) and Thailand (Morley, 2010, 2017).  
558 Although local faults may be misaligned with respect to the regional stress field, at the regional scale,  
559 overall rift kinematics do appear to be compatible with the extension direction (Corti et al., 2007;  
560 Philippon et al., 2015).

561 In contrast to the above interactions, where rift-related faults align with basement shear zones, E-W-  
562 striking shear zones oriented sub-parallel to the extension direction do not directly influence fault  
563 strike. However, these high-angle shear zones are often associated with areas of changing structural  
564 style and segmentation at both the fault and rift scales (Figure 15). At the fault-scale, these high-angle  
565 structures may form boundaries to the lateral propagation of faults (e.g. Duffy et al., 2015; Nixon et  
566 al., 2014), or may transfer strain from one fault to another within a rift (Bladon et al., 2015; Mortimer  
567 et al., 2016). In the northern North Sea, we identify similar interactions, where the Lomre Shear Zone  
568 correlates to a 90° bend along the Vette Fault (Figure 6) (Fazlikhani et al., 2017; Fossen et al., 2016;  
569 Lenhart et al., 2019), whilst the offshore corrugations of the Nordfjord-Sogn Detachment govern fault  
570 and rift architecture across the Måløy Slope (Lenhart et al., 2019).

571 At the rift-scale, shear zones oriented at high angles to the rift may segment rift basins and control the  
572 geometry and distribution of depocentres (see also 'Domain Boundaries' of Fossen et al., 2016). Within

573 the northern North Sea this is particularly important for the distribution of major depocentres during  
574 RP1 and the segmentation of the Viking/Sogn graben system during RP2. The Hardangerfjord Shear  
575 Zone separates the Stord Basin and Åsta Graben (Figure 10a). The Tampen Shear Zone coincides with  
576 the boundary between the North and Central Viking Graben (Figure 10, 13a), whilst further north,  
577 Smethurst (2000) identifies two NW-SE-striking lineaments which bisect the North Viking and Sogn  
578 grabens. Furthermore, the southern continuation of the Lomre Shear Zone projects between the South  
579 and Central Viking grabens and towards the Beryl Embayment (Figure 10, 13b). These structures  
580 oriented at high angles to the rift appear to constrain the length of each rift segment and thus segment  
581 the overall rift.

582 Potential mechanisms for this rift segmentation may include local stress perturbations surrounding the  
583 high-angle structures, as observed in the Turkana depression of the East African rift (Brune et al.,  
584 2017), or the inhibition or retardation of faults at these high-angle structures, as observed offshore  
585 West Greenland (Peace et al., 2017) and along the Atlantic rifted margins (Koopmann et al., 2014).  
586 Where they strike at 45-90° to the regional stress field, Devonian shear zones delineate the main  
587 depocentres during RP1. The Utsira and Hardangerfjord shear zones delineate the main Stord Basin  
588 depocentre (Figure 7, 13), whilst the Tampen, Brent and Ninian shear zones align with and delineate  
589 the main depocentres in the East Shetland Basin (Figure 9, 13). Areas underlain by high-angle shear  
590 zones (oriented 0-45° to the regional extension direction), such as the Viking Graben and Måløy Slope  
591 form less major depocentres during RP1, with the rift-related faults often constrained or segmented by  
592 the pre-existing structures (Figure 15). The presence of Devonian shear zones exerts a strong influence  
593 over the distribution and geometry of rift-related faults and therefore over depocentre geometry, at  
594 least during the initial stage of rifting (Figure 13, 16).

595 The Lomre Shear Zone appears to represent a key structure throughout the evolution of the northern  
596 North Sea, corresponding to the location of strain transfer during RP1 between the Stord Basin along  
597 the eastern rift margin and the East Shetland Basin further north along the western margin, and

598 delineating the eastern boundary to rift activity in RP2 (Figure 13). This structure has an enhanced  
599 influence throughout the multiphase evolution of the rift compared to other interpreted Devonian shear  
600 zones. One possibility is that the Lomre Shear Zone extends to greater (i.e. mid-crustal) depths, or that  
601 it reactivates a Caledonian or earlier structure, both of which have been proposed for the  
602 Hardangerfjord Shear Zone further south, which also exerts a different influence over rift  
603 physiography, being associated with a Moho offset at depth and controlling the location and geometry  
604 of the rift-bounding faults in the Ling Depression (Fossen et al., 2014; Fossen and Hurich, 2005;  
605 Gabrielsen et al., 2015; Maystrenko et al., 2017). The Lomre Shear Zone has been proposed to  
606 represent the southern extension of the Nordfjord-Sogn Detachment by Færseth et al. (1995), although  
607 it does not appear to correlate with the structure onshore (Figure 4).

## 608 **9.2 Strain localization around structural highs**

609 The Utsira High forms a prominent intra-basin high within the northern North Sea, that appears only  
610 weakly faulted throughout RP1 and RP2 (Figure 4, 13). Multiple basement well penetrations across  
611 the Utsira High suggest that, at least in the upper few meters, crystalline basement is granitic  
612 (Fazlikhani et al., 2017; Lundmark et al., 2013; Riber et al., 2015; Slagstad et al., 2011). Granitic  
613 bodies typically have large density and rigidity contrasts with surrounding lithologies, and as such are  
614 often thought to resist extensional stresses and localise strain around their margins (Bott et al., 1958;  
615 Critchley, 1984; de Castro et al., 2007; Howell et al., 2019). The North Pennine and Lake District  
616 batholiths in northern England (Chadwick et al., 1989; Critchley, 1984; Evans et al., 1994; Howell et  
617 al., 2019; Kimbell et al., 2010), as well as granitic bodies interpreted beneath the North Sea (Donato  
618 and Tully, 1982; Donato et al., 1983; Lundmark et al., 2013) typically form structural highs and  
619 appear relatively unaffected by major faulting. Furthermore, at larger scales, numerical modelling has  
620 demonstrated that deformation may localize around the margins of areas of stronger material (Naliboff  
621 and Buitter, 2015; Pascal et al., 2002; Wenker and Beaumont, 2016), as observed with the localization

622 of rifting in orogenic belts surrounding cratonic areas (Daly et al., 1989; Ebinger et al., 1997).  
623 However, the granitic basement beneath the Utsira High likely does not extend to great depths within  
624 the crust as it may be limited by the deeper Utsira Shear Zone (Figure 3b, c, 14). It may be the case the  
625 that the Utsira High is uplifted and exhumed within the footwall of the Utsira Shear Zone in this area,  
626 similar to as observed in core complexes in the North Sea and Barents Sea (Henstra and Rotevatn,  
627 2014; Koehl et al., 2018; Steltenpohl et al., 2004). In addition, strain may localise along the Utsira  
628 Shear Zone during rift activity rather than across the high itself. Regardless of the mechanism of its  
629 formation, the Utsira High represents a long-lived structural high that experienced little internal  
630 deformation during RP1 and RP2, and is underlain by granitic material at shallow basement depths.  
631 We suggest that the presence of this granitic material at shallow basement depths beneath the Utsira  
632 High may inhibit fault nucleation across the structure during RP1. Strain localises around the margins  
633 of the Utsira High, in the adjacent South Viking Graben and Stord Basin during RP1 and solely within  
634 the South Viking Graben during RP2 (Figure 14). Further north, where such granitic material is either  
635 not present, or alternatively not uplifted in the footwall of a shear zone, strain is more uniformly  
636 distributed, forming a single, wide rift (Figure 6, 14b). Although we are unable to directly image the  
637 crustal structure in this area to test this hypothesis, the 3D crustal model of Maystrenko et al. (2017),  
638 although at a relatively coarse resolution, indicates thinned lithosphere beneath the Horda Platform  
639 and slightly thicker lithosphere beneath the Utsira High, in agreement with the model-driven  
640 hypotheses presented here.

641

### 642 **9.3 Migration of rift activity during multiphase rifting**

643 Rift physiography evolves during the multiphase evolution of the northern North Sea rift. Activity  
644 during RP1 is distributed over a wide area, forming a relatively uniform rift. Based on the position of  
645 the main depocentres, the main locus of rift activity passes through the Stord Basin and Northern

646 Horda Platform along the eastern side of the rift, before switching to the western side at the Lomre  
647 Shear Zone and continuing northwards through the East Shetland Basin (Figure 13).

648 During RP2, the location and magnitude of the major depocentres bears less correlation to the location  
649 of Devonian shear zones and rift activity instead localises along the Viking and Sogn grabens, where  
650 crustal thickness is reduced to ~20 km (Figure 14) (Christiansson et al., 2000). This suggests a  
651 decreasing influence from structural inheritance in controlling fault and depocentre geometry during  
652 RP2 (Figure 13). This diminishing influence of discrete basement structures may reflect an increasing  
653 thermal influence associated with the evolving thermal and rheological structure of the lithosphere.  
654 Progressive thinning of the lithosphere during extension is often associated with a narrowing of the  
655 overall rift system as upwelling asthenosphere is increasingly focused into a narrower area. This  
656 localization of lithospheric thinning and rift activity has previously been demonstrated across the north  
657 of the area (i.e. the East Shetland Basin and Northern Horda Platform) through the analysis of crustal-  
658 scale seismic sections (Christiansson et al., 2000; Odinsen et al., 2000). The increasing thermal effects  
659 following lithospheric thinning may cause new rift-related faults to largely ignore pre-existing  
660 structural heterogeneities (Cowie et al., 2005; Odinsen et al., 2000; Paton et al., 2016; Ragon et al.,  
661 2018; Roberts et al., 1995). However, numerical modelling has also shown that, during multiphase  
662 rifting, the lithosphere beneath older rifts may strengthen during inter-rift periods and therefore be less  
663 prone to reactivation during later events (Naliboff and Buiter, 2015). Within the northern North Sea,  
664 we observe an overall localization of the rift system from RP1 to RP2, suggesting that there may not  
665 have been sufficient time between rift phases to sufficiently strengthen the lithosphere, or that  
666 extension was more protracted throughout RP1 and RP2. Observations from the East Shetland Basin  
667 and Oseberg Fault Block indicate that fault activity may continue, albeit at a reduced rate, in the inter-  
668 rift period between RP1 and RP2 (Claringbould et al., 2017; Deng et al., 2017a). However,  
669 strengthening of the lithosphere beneath the RP1 axis in the Stord Basin may also have contributed to

670 the lack of activity in this area during RP2 and the localization of activity in the adjacent South Viking  
671 Graben (Figure 14).

672 During its latter stages, and following RP2, tectonic activity migrated northwards to the NE-SW  
673 trending Marulk and Magnus basins and the Sogn Graben, with little fault activity observed elsewhere  
674 (Figure 11, 13). In addition, faults across the Northern Horda Platform that were not active during  
675 RP2, are active during Late-syn- to Post-RP2 (Figure 11). These faults were diachronously reactivated  
676 from west to east, with those in the west (i.e. towards the Oseberg Fault Block) potentially being  
677 active in the Late Jurassic (Bell et al., 2014). At this time, rift activity within the northern North Sea  
678 lessens and extension in the proto-North Atlantic to the north increases, resulting in a migration of rift  
679 activity northwards and an increase in fault activity in the north of the northern North Sea rift (i.e.  
680 Marulk and Magnus Basins, Sogn Graben) (Coward et al., 2003; Kristoffersen, 1978; Roberts et al.,  
681 1999).

682 Faults across the Northern Horda Platform are also reactivated during Late-syn- to Post-RP2, although  
683 this does not appear to be related to proto-North Atlantic extension as it is further north. Rather, Late-  
684 syn- to Post-RP2 reactivation of faults across the Northern Horda Platform is proposed to be related to  
685 flexural downbending occurring in response to the increase in tectonic activity to the north (Bell et al.,  
686 2014; Brekke and Riis, 1987). This suggests that activity across the Northern Horda Platform during  
687 Late-syn- to Post-RP2 was mainly related to local flexural stresses and that the eastern margin of the  
688 rift (east of the Lomre Shear Zone and Utsira High) was only indirectly influenced by, and largely  
689 remained isolated from regional stresses post-RP1.

690 Although more localised during RP2, rift activity in the north of the study area occurs over roughly the  
691 same area in RP1 and RP2. However, in the south, rifting is localised in the South Viking Graben and  
692 Stord Basin during RP1 and solely the South Viking Graben during RP2, with little activity across the  
693 intervening Utsira High (Figure 14). Extension during RP2 was thought to be at least partly driven by

694 stresses originating from the triple point of the trilete rift system of the Central, Witch Ground and  
695 Viking grabens (Coward et al., 2003; Quirie et al., 2019; Rattey and Hayward, 1993; Underhill and  
696 Partington, 1993). Based on its relative proximity to the origin of this activity, and the potential for  
697 post-RP1 lithospheric strengthening beneath the Stord Basin (Naliboff and Buitter, 2015), we suggest  
698 that upwelling asthenosphere associated with RP2 would be channeled beneath the South Viking  
699 Graben and buttressed by the Utsira High and Lomre Shear Zone to the east, resulting in the Stord  
700 Basin and Northern Horda Platform remaining inactive during RP2 (Figure 14).

## 701 **9.4 Fault interactions during multiphase rifting**

702 Based on the geometry and distribution of syn-rift depocentres, we observe that the N-S-striking faults  
703 across the Northern Horda Platform were active in RP1, inactive during RP2 and later reactivated  
704 during Late-syn- to Post-RP2 (Figures 6, 11, 13). This RP2 inactivity and Late-syn- to Post-RP2  
705 reactivation contrasts with observations across East Shetland Platform, where fault activity is recorded  
706 during RP2 before reducing in Late-syn- to Post-RP2. This reactivation of faults across the Northern  
707 Horda Platform is associated with the formation of NW-SE-striking faults between the main N-S-  
708 striking faults, although these are not resolved in this study (Duffy et al., 2015; Whipp et al., 2014).  
709 These NW-SE-striking faults do not match with the proposed E-W to NW-SW oriented extension  
710 directions proposed for RP2 and are instead proposed to be related to local stress perturbations  
711 surrounding the larger N-S striking faults (Duffy et al., 2015; Reeve et al., 2015; Whipp et al., 2014),  
712 showcasing a similar mechanism to that observed between the shear zones and rift-related faults  
713 during RP1 (Figure 15).

714 In the East Shetland Basin, optimally-aligned (i.e. N-S-striking) RP1 faults were often not reactivated  
715 during RP2 (Claringbould et al., 2017; Tomasso et al., 2008). RP2 extension across the East Shetland  
716 Platform was largely accommodated by the formation of new, mostly E-dipping faults that cross-cut  
717 the pre-existing structures (Figure 9). Claringbould et al. (2017) propose that the lack of reactivation

718 may reflect the increasing influence of thermal effects arising from previously thinned lithosphere,  
719 with the rift narrowing process causing incipient faults to preferentially dip towards the rift axis  
720 (Claringbould et al., 2017; Cowie et al., 2005). A similar process occurs in the East African rift, strain  
721 is initially accommodated over a wide area under the influence of pre-existing structures, before  
722 becoming localised towards the rift axis and neglecting the presence of any pre-existing structures  
723 (Corti, 2009; Ragon et al., 2018).

## 724 **10 Conclusions**

725 In this study we document the regional-scale evolution of the North Sea throughout late Permian-Early  
726 Triassic and Late Jurassic-Early Cretaceous phases of extension. We evaluate how syn-rift depocentres  
727 and their associated normal faults evolve throughout multiple phases of rifting and assess the impact  
728 of structural inheritance.

729 Through documenting the regional-scale multiphase evolution of the northern North Sea rift, and  
730 comparing it to the detailed catalog of pre-existing structural heterogeneities beneath the rift, we show  
731 that:

- 732 1. Rift geometry and activity was highly spatially and temporally variable across the northern  
733 North Sea during late Permian-Early Triassic (RP1) and Late Jurassic-Early Cretaceous (RP2)  
734 rift events.
- 735 2. Extension occurred over a ~200 km wide area during RP1, from the East Shetland Basin to the  
736 Northern Horda Platform in the north and from the South Viking Graben to the Stord Basin in  
737 the south. The location of major depocentres during RP1 appears to have been heavily  
738 influenced by the presence of Devonian basement shear zones, the Utsira Shear zone and  
739 Øygarden/Hardangerfjord Shear zones align with the bounding faults of the Stord Basin,  
740 whilst faults in the East Shetland Basin mirror the geometry and dip direction of the  
741 underlying Tampen, Brent and Ninian shear zones.

- 742 3. Strain is transferred from the Stord Basin/Northern Horda Platform along the eastern margin  
743 of the rift in the south, to the East Shetland Basin along the western rift margin further north.  
744 The site of this strain transfer corresponds to the Lomre Shear Zone.
- 745 4. Rift-related faults may reactivate or align along pre-existing structures such as the Devonian  
746 shear zones either due to the reactivation of internal anisotropies or due to local stress  
747 perturbations around the structure In addition, shear zones situated at high angles to the  
748 regional stress field may be responsible for the segmentation of individual faults and rift  
749 basins, including the Viking Graben.
- 750 5. Rift activity localises onto the Viking and Sogn grabens during RP2, with negligible  
751 reactivation of structures along the eastern rift margin, i.e. the Stord Basin and Northern Horda  
752 Platform and activity along structures in the East Shetland Basin. The eastern margin of  
753 activity during RP2 is delineated by the Utsira High in the south and the Lomre Shear zone  
754 further north.
- 755 6. As extension in the northern North Sea wanes during the latter stages of RP2, rift activity  
756 migrates northwards towards the Sogn Graben and the Marulk and Magnus Basins. This  
757 migration of rift activity reflects extension related to the opening of the North Atlantic Ocean  
758 becoming the dominant regional stress. Increased rift activity in the north of the study area  
759 drives the local flexural reactivation of faults across the Northern Horda Platform.
- 760 7. The Utsira High represents a long-lived structural high that resists extension throughout RP1  
761 and RP2. Following RP1, we propose that increased lithospheric thickness was preserved  
762 beneath the Utsira High with thinned lithosphere beneath the Stord Basin and South Viking  
763 Graben. As a result, we suggest that activity during RP2 was focused beneath the South  
764 Viking Graben and pinned eastwards at the Utsira High and Lomre Shear zone, causing the  
765 Stord Basin and Northern Horda Platform to the east to largely remain inactive.

766 8. The influence of pre-existing structural heterogeneities, here represented primarily by  
767 Devonian shear zones, exert a diminished influence over rift physiography during later rift  
768 phases. Although they delineate the boundary to activity during RP2, they do not control the  
769 main depocentres. The Viking Graben instead appears to be more influenced by modification  
770 of the lithospheric structure associated with the earlier phase of rifting.

771 We highlight how structural inheritance and multiple phases of rifting influence the regional geometry  
772 and evolution of rift systems. Pre-existing structural heterogeneities that are relatively well-aligned  
773 with the rift dictate the initial geometry of major rift-related faults and their associated syn-rift  
774 depocentres, whilst those oriented at relatively high-angles to the rift may segment faults and rifts.  
775 Furthermore, we show how rift activity migrates and localises across the rift during multiple phases of  
776 rifting, showing a decreased influence from structural inheritance and an increased role from thermal  
777 effects associated with prior phases of lithospheric thinning. However, pre-existing structures still  
778 exert some control over rift physiography and kinematics during these later events, determining the  
779 areas of rift activity and whether certain faults will be reactivated.

780

## 781 **Figure captions**

782 Figure 1 – Regional setting of the North Sea between the UK and Norway. The northern North Sea rift  
783 (NNS) study area is shown by the red rectangle. The locations of major lineaments identified onshore  
784 and offshore are marked by thick black lines after Fazlikhani et al. (2017). Onshore Norway basement  
785 geology from Fossen et al. (2016); gray areas correspond to Caledonian nappes, beige colors represent  
786 Proterozoic-aged basement whilst yellow colors indicate Devonian basins. The main offshore rift axes  
787 are shown in orange. MTFC – Møre-Trondelag Fault Complex; WGR – Western Gneiss Region;  
788 NSDZ – Nordfjord-Sogn Detachment Zone; BASZ – Bergen Arc Shear Zone; HSZ – Hardangerfjord

789 Shear Zone; KSZ – Karmøy Shear Zone; SSZ – Stavanger Shear Zone; STZ – Sorgenfrei-Tornquist  
790 Zone.

791 Figure 2 – Regional stratigraphic columns across various sub-basins of the northern North Sea rift,  
792 showing the different lithostratigraphic units that comprise temporally consistent surfaces referred to  
793 and mapped throughout this study. Compiled from Patruno and Reid (2016) and NPD (2014).

794 Figure 3– Regional seismic sections across the northern North Sea rift from north to south. See Figure  
795 1 for section locations and see appendix for uninterpreted sections. A) Interpreted seismic section  
796 stretching from the East Shetland Basin in the east to the Northern Horda Platform in the west. Key  
797 surfaces and structures referred to in this study are identified. B) Interpreted seismic section across the  
798 central portion of the rift, from the Central Viking Graben to the Stord Basin. Note the presence of  
799 Devonian basins beneath the pre-rift surface on the East Shetland Platform and the identification of the  
800 Utsira Shear zone and the Hardangerfjord and Øygarden shear zones beneath the northern Utsira High  
801 and Stord Basin respectively. C) Interpreted seismic section across the southern portion of the rift,  
802 stretching from the South Viking Graben to the Åsta Graben and Stavanger Platform. Pre-rift strata of  
803 Carboniferous-Permian age are identified beneath the Ling Depression, Sele High and Åsta Graben,  
804 with the Utsira and Karmøy shear zones present beneath the Utsira High and Åsta Graben/Stavanger  
805 Platform respectively. Note that the Utsira High forms a series of sub-horizontal to E-dipping strands  
806 in this area. Data courtesy of TGS (A - NSR06-31182.0009614; B - NSR06-31154.0015823; C -  
807 NSR05-211321.0015647).

808 Figure 4 – Two-way-time structure map of the Base RP1 structure map, modified after Fazlikhani et  
809 al. (2017). See Figures 2 and 3 for structural level. The offshore extensions of Devonian shear zones  
810 are shown by white translucent lines (after Fazlikhani et al. 2017), with those referred to in the study  
811 labelled in gray. The Utsira High forms an intra-basinal high in the south of the area. The pink line  
812 represents the limit of mobile salt of the Zechstein Supergroup. Major structural lows include the Stord

813 Basin, East Shetland Basin and the Viking Graben and Sogn Graben. Faults: WBF – Western  
814 Boundary Fault; ØF (S/C/N) – Øygarden Fault (South/Central/North); ÅF – Åsta Fault. Shear Zones:  
815 NSZ – Ninian Shear Zone; BSZ - Brent Shear Zone; TSZ – Tampen Shear Zone; LSZ – Lomre Shear  
816 Zone; USZ – Utsira Shear Zone; HSZ – Hardangerfjord Shear Zone; KSZ – Karmøy Shear Zone; SSZ  
817 – Stavanger Shear Zone.

818 Figure 5 – TWT structure maps of shallower structural levels, see Figures 2 and 3 for equivalent  
819 stratigraphic horizons. A) TWT structure map of the Middle Jurassic (Base RP2) surface. The main  
820 structural lows are the South, Central, North Viking Graben and the Sogn Graben, deepening to the  
821 north. B) TWT structure map of the Base Cretaceous Unconformity (Near Top-RP2) horizon, showing  
822 the main structural lows in the Viking Graben. Note the additional low centred above the Stord Basin.  
823 C) TWT structure map of the Top Cretaceous (Post-rift) surface. This surface shows little faulting  
824 aside from the Western Boundary Fault along its western margin and is dominated by a N-trending  
825 depression, which widens northwards.

826 Figure 6 – Time-thickness map for Rift Phase 1, calculated between the Base RP1 and Base RP2  
827 surfaces. Calculated depocentres are shown on the left and interpretation on the right. Red lines show  
828 the location of the offshore extensions of major Devonian structures (after Fazlikhani et al. (2017)).  
829 NSZ – Ninian Shear Zone; BSZ – Brent Shear Zone; TSZ – Tampen Shear Zone; LSZ – Lomre Shear  
830 Zone; USZ – Utsira Shear Zone; ØSZ – Øygarden Shear Zone; HSZ – Hardangerfjord Shear Zone;  
831 KSZ – Karmøy Shear Zone; WBF – Western Boundary Fault; TF – Tusse Fault; VF – Vette Fault; ØF  
832 (C and S) – Øygarden Fault (Central and Southern); ÅF - Åsta Fault

833 Figure 7 – Uninterpreted and interpreted seismic section across the Stord Basin, see Figure 4 for  
834 location. The section shows major RP1 activity along basin-bounding faults, which appear to root  
835 down onto the underlying Utsira and Øygarden/Hardangerfjord Shear zones at depth. Westwards

836 progradation of the Hardangerfjord Delta can be observed in the Jurassic. Data courtesy of TGS  
837 (NSR06-31158.0016678).

838 Figure 8 – Uninterpreted and interpreted seismic section across the Northern Horda Platform, see  
839 Figure 4 for location. The W-dipping Tusse, Vette and Øygarden Faults show activity in the Triassic  
840 (RP1) and Cretaceous (Late-syn- to Post-RP2) with no activity in the Late Jurassic (RP2). The  
841 Øygarden and Vette Faults also show evidence of reflectivity below the Base RP1 surface. Data  
842 courtesy of TGS (NSR06-31182.0009614).

843 Figure 9 – Uninterpreted and interpreted section from across the East Shetland Basin, see Figure 4 for  
844 location. E-dipping faults appear to merge beneath the East Shetland Basin and may link to the  
845 Tampen and Ninian shear zones in this area. The depth to the Base RP1 surface becomes uncertain to  
846 the east, beneath the North Viking Graben. Data courtesy of TGS (NSR06-21188.0010680)

847 Figure 10 – Time-thickness and activity maps for RP2, calculated between the Base RP2 and BCU  
848 (Near Top-RP2) surfaces. Dashed diagonal lines correspond to areas of non-deposition or erosion.  
849 Green lines represent the offshore location of Devonian shear zones, with structures referred to in the  
850 text labelled. The Upper Jurassic Hardangerfjord and Sognefjord deltaic sequences are shown in  
851 brown. TSZ – Tampen Shear Zone; LSZ – Lomre Shear Zone; WBF – Western Boundary Fault; VF –  
852 Vette Fault.

853 Figure 11 – Time-thickness map for Late-syn- to Post-RP2, calculated between the BCU (Near Top-  
854 RP2) and top Lower Cretaceous (Post-rift) surfaces. Devonian shear zones are highlighted by light  
855 blue lines. The thickness of strata increases northwards into the Sogn Graben and Marulk and Magnus  
856 Basins. Note the reactivation of the faults across the Northern Horda Platform. TSZ – Tampen Shear  
857 Zone; LSZ – Lomre Shear Zone; WBF – Western Boundary Fault; TF – Tusse Fault; VF – Vette  
858 Fault; ØF (C) – Øygarden Fault (Central).

859 Figure 12 – Uninterpreted and interpreted seismic sections across the Sogn Graben, see Figure 4 for  
860 location. The Sogn Graben displays some activity during RP1 but is mainly active in RP2. The  
861 eastern margin of the graben is active during RP2 and Late-syn- to Post-RP2 intervals. No RP1 strata  
862 are present across the Måløy Slope, which shows RP2 activity. Data courtesy of CGG (Horda Platform  
863 Broadband 3D seismic volume)

864 Figure 13 – Regional model for the multiphase evolution of the northern North Sea rift. A) Major RP1  
865 depocentres in the Stord Basin and East Shetland Basin are delineated by and somewhat controlled by  
866 the Devonian shear zones. B) RP2 activity localises onto the Viking and Sogn Grabens and the East  
867 Shetland Basin, with negligible activity observed across the Stord Basin and Northern Horda Platform,  
868 east of the Utsira High and the Lomre Shear Zone. C) Rift activity migrates northwards during the  
869 later stages and following RP2. Activity occurs along the NE-trending Marulk and Magnus Basins in  
870 the north of the area with local flexure related reactivation of faults across the Northern Horda  
871 Platform.

872 Figure 14 – Schematic model showing the difference in activity between the northern and southern  
873 sections of the study area, and the role of the Utsira High. A) During RP1, rift activity in the north is  
874 distributed over a wide area, forming a wide rift and resulting in uniform lithospheric thinning. In the  
875 south, extension is localised into two segments either side of the relatively unfaulted Utsira High,  
876 producing relatively thin lithosphere beneath the rift segments and leaving relatively thicker  
877 lithosphere beneath the Utsira High. Question marks reflect the uncertainty associated with the nature  
878 of basement at greater depths beneath the Utsira High. B) During RP2, the uniformly thinned  
879 lithosphere in the north focusses activity towards the axis, creating a localised rift centred across the  
880 Viking Graben. Estimated crustal thicknesses in the northern model are taken from Christiansson et al.  
881 (2000). In the south, the modified lithospheric structure remnant from RP1 focusses activity along one  
882 rift segment, the South Viking Graben, buttressed by the thicker lithosphere of the Utsira High; whilst  
883 the rift segment on the opposite side to the Utsira High, the Stord Basin, becomes abandoned.

884 Figure 15 – 3D box model highlighting the range of possible interactions between pre-existing  
885 basement structures and rift related faults throughout multiple rift phases. Shear zones may locally  
886 perturb the regional stress field, causing incipient faults to locally align along these structures. Faults  
887 may also exploit internal anisotropies within shear zones, or where the shear zones are oriented at a  
888 relatively high angle, be segmented by them. In some instances, shear zones may form the limit to  
889 activity during later rift events. Granite-cored bodies are often located in the footwalls of faults and are  
890 typically resistant to extension.

891 Figure S1 – Uninterpreted seismic sections of Figure 3.

892 Table A1 – Summary of seismic surveys and their acquisition parameters as used in this study. From  
893 Fazlikhani et al. (2017).

894 Table A2 – Table showing basement penetrating exploration wells used in this study, after Fazlikhani  
895 et al. (2017). Depths shown are measured depth (MD) from the Kelly Bushing (KB) datum. Well  
896 information shown by asterisk is from Bassett (2003) and Marshall and Hewett (2003).

## 897 **Acknowledgements**

898 This contribution forms part of the MultiRift Project funded by the Research Council of Norway  
899 (PETROMAKS project215591/E30) and Equinor to the University of Bergen and partners Imperial  
900 College, University of Manchester and University of Oslo. Uninterpreted versions of the seismic  
901 sections shown in this study are available in the supplementary material. The seismic data used in this  
902 study are publically available for download via the DISKOS online portal  
903 (<https://portal.diskos.cgg.com>). Thanks to TGS and CGG for permission to publish the seismic data  
904 and to Schlumberger for providing academic licenses for the use of Petrel at the University of Bergen  
905 and the University of Durham. We would also like to thank the VISTA program for supporting the  
906 professorship of Gawthorpe and visiting researcher scholarships to Phillips at the University of Bergen

907 in 2018 and 2019. We also thank the Leverhulme Trust for supporting Phillips through a Leverhulme  
908 Early Career Fellowship at the University of Durham. Two anonymous reviewers are thanked for their  
909 constructive comments which improved the manuscript, as well as Laurent Jolivet for editorial  
910 handling. Additional members of the MultiRift project are thanked for fruitful discussions throughout  
911 the project.

912

913

914

915

916

917

918

919

920

921

## 922 **References**

923 (BIRPS), B.I.R.P.S., (ECORS), E.d.I.C.C.e.O.p.R.e.R.S., 1986. Deep seismic reflection profiling between  
924 England, France and Ireland. *Journal of the Geological Society, London* 143, 45-52.

925 Andersen, T.B., Jamtveit, B., 1990. Uplift of deep crust during orogenic extensional collapse: A model  
926 based on field studies in the Sogn-Sunnfjord Region of western Norway. *Tectonics* 9, 1097-1111.

927 Bartholomew, I.D., Peters, J.M., Powell, C.M., 1993. Regional structural evolution of the North Sea:  
928 oblique slip and the reactivation of basement lineaments. *Geological Society, London, Petroleum*  
929 *Geology Conference series* 4, 1109-1122.

- 930 Bassett, M., 2003. Sub-Devonian geology, in: Evans, D., Graham, C., Armour, D., Bathurst, P. (Eds.),  
931 The Millennium Atlas: Petroleum Geology of the Central and Northern North Sea. The Geological  
932 Society of London, pp. 61-63.
- 933 Bell, R.E., Jackson, C.A.L., Whipp, P.S., Clements, B., 2014. Strain migration during multiphase  
934 extension: Observations from the northern North Sea. *Tectonics* 33, 1936-1963.
- 935 Bird, P.C., Cartwright, J.A., Davies, T.L., 2014. Basement reactivation in the development of rift  
936 basins: an example of reactivated Caledonide structures in the West Orkney Basin. *Journal of the  
937 Geological Society* 172, 77-85.
- 938 Bladon, A.J., Clarke, S.M., Burley, S.D., 2015. Complex rift geometries resulting from inheritance of  
939 pre-existing structures: Insights and regional implications from the Barmer Basin rift. *Journal of  
940 Structural Geology* 71, 136-154.
- 941 Bøe, R., Fossen, H., Smelror, M., 2010. Mesozoic sediments and structures onshore Norway and in  
942 the coastal zone. *Norges geologiske undersøkelse Bulletin* 450, 15-32.
- 943 Boone, S.C., Seiler, C., Kohn, B.P., Gleadow, A.J.W., Foster, D.A., Chung, L., 2018. Influence of Rift  
944 Superposition on Lithospheric Response to East African Rift System Extension: Lapur Range, Turkana,  
945 Kenya. *Tectonics* 37, 182-207.
- 946 Bott, M.H.P., Day, A.A., Masson-Smith, D., 1958. The Geological Interpretation of Gravity and  
947 Magnetic Surveys in Devon and Cornwall. *Philos Tr R Soc S-A* 251, 161-191.
- 948 Brekke, H., Riis, F., 1987. Tectonics and basin evolution of the Norwegian shelf between 62 N and 72  
949 N. *Norsk geologisk tidsskrift* 67, 295-322.
- 950 Brun, J.P., Tron, V., 1993. Development of the North Viking Graben - Inferences from Laboratory  
951 Modeling. *Sedimentary Geology* 86, 31-51.
- 952 Brune, S., Corti, G., Ranalli, G., 2017. Controls of inherited lithospheric heterogeneity on rift linkage:  
953 Numerical and analog models of interaction between the Kenyan and Ethiopian rifts across the  
954 Turkana depression. *Tectonics* 36, 1767-1786.
- 955 Chadwick, R.A., Pharaoh, T.C., Smith, N.J.P., 1989. Lower crustal heterogeneity beneath Britain from  
956 deep seismic reflection data. *Journal of the Geological Society* 146, 617.
- 957 Chattopadhyay, A., Chakra, M., 2013. Influence of pre-existing pervasive fabrics on fault patterns  
958 during orthogonal and oblique rifting: An experimental approach. *Marine and Petroleum Geology* 39,  
959 74-91.
- 960 Christiansson, P., Faleide, J.I., Berge, A.M., 2000. Crustal structure in the northern North Sea: an  
961 integrated geophysical study. Geological Society, London, Special Publications 167, 15.
- 962 Claringbould, J.S., Bell, R.E., Jackson, C.A.L., Gawthorpe, R.L., Odinsen, T., 2017. Pre-existing normal  
963 faults have limited control on the rift geometry of the northern North Sea. *Earth and Planetary  
964 Science Letters*.

- 965 Collanega, L., Jackson, C.A.L., Bell, R.E., Coleman, A.J., Lenhart, A., Breda, A., 2018. Normal fault  
966 growth influenced by basement fabrics: the importance of preferential nucleation from pre-existing  
967 structures. *Basin Res* 0.
- 968 Corti, G., 2008. Control of rift obliquity on the evolution and segmentation of the main Ethiopian rift.  
969 *Nature Geoscience* 1, 258.
- 970 Corti, G., 2009. Continental rift evolution: From rift initiation to incipient break-up in the Main  
971 Ethiopian Rift, East Africa. *Earth-Science Reviews* 96, 1-53.
- 972 Corti, G., van Wijk, J., Cloetingh, S., Morley, C.K., 2007. Tectonic inheritance and continental rift  
973 architecture: Numerical and analogue models of the East African Rift system. *Tectonics* 26.
- 974 Coward, M.P., 1990. The Precambrian, Caledonian and Variscan framework to NW Europe. Geological  
975 Society, London, Special Publications 55, 1-34.
- 976 Coward, M.P., 1995. Structural and tectonic setting of the Permo-Triassic basins of northwest  
977 Europe. Geological Society, London, Special Publications 91, 7-39.
- 978 Coward, M.P., Dewey, J.F., Hempton, M., Holroyd, J., 2003. Tectonic evolution, in: Evans, D., Graham,  
979 C., Armour, A., Bathurst, P. (Eds.), *The Millenium Atlas: petroleum geology of the central and*  
980 *northern North Sea*, Geological Society of London.
- 981 Cowie, P.A., Underhill, J.R., Behn, M.D., Lin, J., Gill, C.E., 2005. Spatio-temporal evolution of strain  
982 accumulation derived from multi-scale observations of Late Jurassic rifting in the northern North Sea:  
983 A critical test of models for lithospheric extension. *Earth and Planetary Science Letters* 234, 401-419.
- 984 Critchley, M.F., 1984. Variscan tectonics of the Alston block, northern England. Geological Society,  
985 London, Special Publications 14, 139.
- 986 Daly, M.C., Chorowicz, J., Fairhead, J.D., 1989. Rift basin evolution in Africa: the influence of  
987 reactivated steep basement shear zones. Geological Society, London, Special Publications 44, 309.
- 988 Davies, R.J., O'Donnell, D., Bentham, P.N., Gibson, J.P.C., Curry, M.R., Dunay, R.E., Maynard, J.R.,  
989 1999. The origin and genesis of major Jurassic unconformities within the triple junction area of the  
990 North Sea, UK. Geological Society, London, Petroleum Geology Conference series 5, 117.
- 991 Davies, R.J., Turner, J.D., Underhill, J.R., 2001. Sequential dip-slip fault movement during rifting: a  
992 new model for the evolution of the Jurassic trilete North Sea rift system. *Petroleum Geoscience* 7,  
993 371.
- 994 de Castro, D.L., de Oliveira, D.C., Gomes Castelo Branco, R.M., 2007. On the tectonics of the  
995 Neocomian Rio do Peixe Rift Basin, NE Brazil: Lessons from gravity, magnetics, and radiometric data.  
996 *Journal of South American Earth Sciences* 24, 184-202.
- 997 Deng, C., Fossen, H., Gawthorpe, R.L., Rotevatn, A., Jackson, C.A.L., FazliKhani, H., 2017a. Influence of  
998 fault reactivation during multiphase rifting: The Oseberg area, northern North Sea rift. *Marine and*  
999 *Petroleum Geology* 86, 1252-1272.

- 1000 Deng, C., Gawthorpe, R.L., Finch, E., Fossen, H., 2017b. Influence of a pre-existing basement  
1001 weakness on normal fault growth during oblique extension: Insights from discrete element modeling.  
1002 *Journal of Structural Geology*.
- 1003 Donato, J., Tully, M., 1982. A proposed granite batholith along the western flank of the North Sea  
1004 Viking Graben. *Geophysical Journal International* 69, 187-195.
- 1005 Donato, J.A., Martindale, W., Tully, M.C., 1983. Buried granites within the Mid North Sea High.  
1006 *Journal of the Geological Society* 140, 825.
- 1007 Dore, A.G., Lundin, E.R., Fichler, C., Olesen, O., 1997. Patterns of basement structure and reactivation  
1008 along the NE Atlantic margin. *Journal of the Geological Society* 154, 85-92.
- 1009 Dreyer, T., Whitaker, M., Dexter, J., Flesche, H., Larsen, E., 2005. From spit system to tide-dominated  
1010 delta: integrated reservoir model of the Upper Jurassic Sognefjord Formation on the Troll West Field.  
1011 *Geological Society, London, Petroleum Geology Conference* series 6, 423.
- 1012 Duffy, O.B., Bell, R.E., Jackson, C.A.L., Gawthorpe, R.L., Whipp, P.S., 2015. Fault growth and  
1013 interactions in a multiphase rift fault network: Horda Platform, Norwegian North Sea. *Journal of*  
1014 *Structural Geology* 80, 99-119.
- 1015 Ebinger, C., Djomani, Y.P., Mbede, E., Foster, A., Dawson, J.B., 1997. Rifting Archaean lithosphere: the  
1016 Eyasi-Manyara-Natron rifts, East Africa. *Journal of the Geological Society* 154, 947.
- 1017 Evans, D., Graham, C., Armour, A., Bathurst, P., 2003. *The Millennium Atlas: Petroleum Geology of*  
1018 *the Central and Northern North Sea. The Geological Society of London.*
- 1019 Evans, D.J., Rowley, W.J., Chadwick, R.A., Kimbell, G.S., Millward, D., 1994. Seismic reflection data  
1020 and the internal structure of the Lake District batholith, Cumbria, northern England. *Proceedings of*  
1021 *the Yorkshire Geological and Polytechnic Society* 50, 11.
- 1022 Færseth, R.B., 1996. Interaction of Permo-Triassic and Jurassic extensional fault-blocks during the  
1023 development of the northern North Sea. *Journal of the Geological Society* 153, 931-944.
- 1024 Færseth, R.B., Gabrielsen, R.H., Hurich, C.A., 1995. Influence of basement in structuring of the North  
1025 Sea basin, offshore southwest Norway. *Norsk Geologisk Tidsskrift* 75, 105-119.
- 1026 Færseth, R.B., Knudsen, B.E., Liljedahl, T., Midbøe, P.S., Sjøderstrøm, B., 1997. Oblique rifting and  
1027 sequential faulting in the Jurassic development of the northern North Sea. *Journal of Structural*  
1028 *Geology* 19, 1285-1302.
- 1029 Færseth, R.B., Ravnås, R., 1998. Evolution of the Oseberg fault-block in context of the northern north  
1030 sea structural framework. *Marine and Petroleum Geology* 15, 467-490.
- 1031 Fazlikhani, H., Fossen, H., Gawthorpe, R., Faleide, J.I., Bell, R.E., 2017. Basement structure and its  
1032 influence on the structural configuration of the northern North Sea rift. *Tectonics* 36, 1151-1177.

- 1033 Fichler, C., Odinsen, T., Rueslåtten, H., Olesen, O., Vindstad, J.E., Wienecke, S., 2011. Crustal  
1034 inhomogeneities in the Northern North Sea from potential field modeling: Inherited structure and  
1035 serpentinites? *Tectonophysics* 510, 172-185.
- 1036 Fossen, H., 1992. The role of extensional tectonics in the Caledonides of south Norway. *Journal of*  
1037 *Structural Geology* 14, 1033-1046.
- 1038 Fossen, H., 2010. Extensional tectonics in the North Atlantic Caledonides: a regional view. *Geological*  
1039 *Society, London, Special Publications* 335, 767-793.
- 1040 Fossen, H., Dunlap, J.W., 1998. Timing and kinematics of Caledonian thrusting and extensional  
1041 collapse, southern Norway: evidence from <sup>40</sup>Ar/<sup>39</sup>Ar thermochronology. *Journal of Structural*  
1042 *Geology* 20, 765-781.
- 1043 Fossen, H., Dunlap, W.J., 1999. On the age and tectonic significance of Permo-Triassic dikes in the  
1044 Bergen-Sunnhordland region, southwestern Norway. *Norsk Geologisk Tidsskrift* 79, 169-178.
- 1045 Fossen, H., Gabrielsen, R.H., Faleide, J.I., Hurich, C.A., 2014. Crustal stretching in the Scandinavian  
1046 Caledonides as revealed by deep seismic data. *Geology* 42, 791-794.
- 1047 Fossen, H., Hurich, C.A., 2005. The Hardangerfjord Shear Zone in SW Norway and the North Sea: a  
1048 large-scale low-angle shear zone in the Caledonian crust. *Journal of the Geological Society* 162, 675-  
1049 687.
- 1050 Fossen, H., Khani, H.F., Faleide, J.I., Ksienzyk, A.K., Dunlap, W.J., 2016. Post-Caledonian extension in  
1051 the West Norway–northern North Sea region: the role of structural inheritance. *Geological Society,*  
1052 *London, Special Publications* 439.
- 1053 Fossen, H., Rykkelid, E., 1992. Postcollisional extension of the Caledonide orogen in Scandinavia:  
1054 Structural expressions and tectonic significance. *Geology* 20, 737.
- 1055 Gabrielsen, R.H., Fossen, H., Faleide, J.I., Hurich, C.A., 2015. Mega-scale Moho relief and the structure  
1056 of the lithosphere on the eastern flank of the Viking Graben, offshore southwestern Norway.  
1057 *Tectonics* 34, 803-819.
- 1058 Gabrielsen, R.H., Kyrkjebø, R., Faleide, J.I., Fjeldskaar, W., Kjennerud, T., 2001. The Cretaceous post-  
1059 rift basin configuration of the northern North Sea. *Petroleum Geoscience* 7, 137-154.
- 1060 Gee, D.G., Fossen, H., Henriksen, N., Higgins, A.K., 2008. From the early Paleozoic platforms of Baltica  
1061 and Laurentia to the Caledonide Orogen of Scandinavia and Greenland. *Episodes* 31, 44-51.
- 1062 Gontijo-Pascutti, A., Bezerra, F.H.R., Terra, E.L., Almeida, J.C.H., 2010. Brittle reactivation of mylonitic  
1063 fabric and the origin of the Cenozoic Rio Santana Graben, southeastern Brazil. *Journal of South*  
1064 *American Earth Sciences* 29, 522-536.
- 1065 Heeremans, M., Faleide, J.I., 2004. Late Carboniferous-Permian tectonics and magmatic activity in the  
1066 Skagerrak, Kattegat and the North Sea. *Geological Society, London, Special Publications* 223, 157-176.

- 1067 Heeremans, M., Faleide, J.I., Larsen, B.T., 2004. Late Carboniferous -Permian of NW Europe: an  
1068 introduction to a new regional map. *Geol Soc London, Special Publication 223*, 75-88.
- 1069 Heilman, E., Kolawole, F., Atekwana, E.A., Mayle, M., 2019. Controls of Basement Fabric on the  
1070 Linkage of Rift Segments. *Tectonics* 0.
- 1071 Henstra, G.A., Berg Kristensen, T., Rotevatn, A., Gawthorpe, R.L., 2019. How do pre-existing normal  
1072 faults influence rift geometry? A comparison of adjacent basins with contrasting underlying structure  
1073 on the Lofoten Margin, Norway. *Basin Res* 0.
- 1074 Henstra, G.A., Rotevatn, A., 2014. Nature of Palaeozoic extension in Lofoten, north Norwegian  
1075 Continental Shelf: insights from 3-D seismic analysis of a Cordilleran-style metamorphic core  
1076 complex. *Terra Nova* 26, 247-252.
- 1077 Henstra, G.A., Rotevatn, A., Gawthorpe, R.L., Ravnås, R., 2015. Evolution of a major segmented  
1078 normal fault during multiphase rifting: The origin of plan-view zigzag geometry. *Journal of Structural  
1079 Geology* 74, 45-63.
- 1080 Hossack, J.R., Cooper, M.A., 1986. Collision tectonics in the Scandinavian Caledonides. *Geological  
1081 Society, London, Special Publications* 19, 285-304.
- 1082 Howell, L., Egan, S., Leslie, G., Clarke, S., 2019. Structural and geodynamic modelling of the influence  
1083 of granite bodies during lithospheric extension: Application to the Carboniferous basins of northern  
1084 England. *Tectonophysics*.
- 1085 Hurich, C., Kristoffersen, Y., 1988. Deep structure of the Caledonide orogen in southern Norway: new  
1086 evidence from marine seismic reflection profiling. *Norges Geologiske Undersøkelse Special  
1087 Publication* 3, 96-101.
- 1088 Jackson, C.A.L., Lewis, M.M., 2013. Physiography of the NE margin of the Permian Salt Basin: new  
1089 insights from 3D seismic reflection data. *Journal of the Geological Society* 170, 857-860.
- 1090 Jackson, C.A.L., Lewis, M.M., 2016. Structural style and evolution of a salt-influenced rift basin  
1091 margin; the impact of variations in salt composition and the role of polyphase extension. *Basin Res*  
1092 28, 81-102.
- 1093 Jackson, C.A.L., Stewart, S.A., 2017. Chapter 8 - Composition, Tectonics, and Hydrocarbon  
1094 Significance of Zechstein Supergroup Salt on the United Kingdom and Norwegian Continental  
1095 Shelves: A Review, in: Soto, J.I., Flinch, J.F., Tari, G. (Eds.), *Permo-Triassic Salt Provinces of Europe,  
1096 North Africa and the Atlantic Margins*. Elsevier, pp. 175-201.
- 1097 Kimbell, G.S., Young, B., Millward, D., Crowley, Q.G., 2010. The North Pennine batholith (Weardale  
1098 Granite) of northern England: new data on its age and form. *Proceedings of the Yorkshire Geological  
1099 Society* 58, 107.
- 1100 Kirkpatrick, J.D., Bezerra, F.H.R., Shipton, Z.K., Do Nascimento, A.F., Pytharouli, S.I., Lunn, R.J., Soden,  
1101 A.M., 2013. Scale-dependent influence of pre-existing basement shear zones on rift faulting: a case  
1102 study from NE Brazil. *Journal of the Geological Society* 170, 237.

- 1103 Klemperer, S., Hobbs, R., 1991. The BIRPS Atlas: Deep seismic reflection profiles around the British  
1104 Isles. Cambridge University Press.
- 1105 Koehl, J.B.P., Bergh, S.G., Henningsen, T., Faleide, J.I., 2018. Middle to Late Devonian–Carboniferous  
1106 collapse basins on the Finnmark Platform and in the southwesternmost Nordkapp basin, SW Barents  
1107 Sea. *Solid Earth* 9, 341-372.
- 1108 Koopmann, H., Brune, S., Franke, D., Breuer, S., 2014. Linking rift propagation barriers to excess  
1109 magmatism at volcanic rifted margins. *Geology* 42, 1071-1074.
- 1110 Kristoffersen, Y., 1978. Sea-floor spreading and the early opening of the North Atlantic. *Earth and  
1111 Planetary Science Letters* 38, 273-290.
- 1112 Kyrkjebø, R., Gabrielsen, R., Faleide, J., 2004. Unconformities related to the Jurassic–Cretaceous  
1113 synrift–post-rift transition of the northern North Sea. *Journal of the Geological Society* 161, 1-17.
- 1114 Lenhart, A., Jackson, C.A.L., Bell, R.E., Duffy, O.B., Gawthorpe, R.L., Fossen, H., 2019. Structural  
1115 architecture and composition of crystalline basement offshore west Norway. *Lithosphere-U* 11, 273-  
1116 293.
- 1117 Lundmark, A.M., Saether, T., Sorlie, R., 2013. Ordovician to Silurian magmatism on the Utsira High,  
1118 North Sea: implications for correlations between the onshore and offshore Caledonides. *Geological  
1119 Society, London, Special Publications* 390, 513-523.
- 1120 Marshall, J., Hewett, T., 2003. Devonian, in: Evans, D., Graham, C., Armour, A., Bathurst, P. (Eds.), *The  
1121 Millenium Atlas: Petroleum Geology of the Central and Northern North Sea*. Geological Society of  
1122 London, pp. 6-16.
- 1123 Maystrenko, Y.P., Olesen, O., Ebbing, J., Nasuti, A., 2017. Deep structure of the northern North Sea  
1124 and southwestern Norway based on 3D density and magnetic modelling. *Norwegian Journal of  
1125 Geology/Norsk Geologisk Forening* 97.
- 1126 McClay, Norton, M.G., Coney, P., Davis, G.H., 1986. Collapse of the Caledonian orogen and the Old  
1127 Red Sandstone. *Nature* 323, 147-149.
- 1128 McKerrow, W.S., MacNiocaill, C., Dewey, J.F., 2000. The Caledonian Orogeny redefined. *Journal of  
1129 the Geological Society, London* 157, 1149-1154.
- 1130 Milnes, A.G., Wennberg, O.P., Skår, Ø., Koestler, A.G., 1997. Contraction, extension and timing in the  
1131 South Norwegian Caledonides: the Sognefjord transect. *Geological Society, London, Special  
1132 Publications* 121, 123.
- 1133 Morley, C.K., 2010. Stress re-orientation along zones of weak fabrics in rifts: An explanation for pure  
1134 extension in ‘oblique’ rift segments? *Earth and Planetary Science Letters* 297, 667-673.
- 1135 Morley, C.K., 2017. The impact of multiple extension events, stress rotation and inherited fabrics on  
1136 normal fault geometries and evolution in the Cenozoic rift basins of Thailand. *Geological Society,  
1137 London, Special Publications* 439, 413.

- 1138 Morley, C.K., Haranya, C., Phoosongsee, W., Pongwapee, S., Kornsawan, A., Wonganan, N., 2004.  
1139 Activation of rift oblique and rift parallel pre-existing fabrics during extension and their effect on  
1140 deformation style: examples from the rifts of Thailand. *Journal of Structural Geology* 26, 1803-1829.
- 1141 Mortimer, E.J., Paton, D.A., Scholz, C.A., Strecker, M.R., 2016. Implications of structural inheritance in  
1142 oblique rift zones for basin compartmentalization: Nkhata Basin, Malawi Rift (EARS). *Marine and  
1143 Petroleum Geology* 72, 110-121.
- 1144 Naliboff, J., Buiter, S.J., 2015. Rift reactivation and migration during multiphase extension. *Earth and  
1145 Planetary Science Letters* 421, 58-67.
- 1146 Neumann, E.-R., Wilson, M., Heeremans, M., Spencer, E.A., Obst, K., Timmerman, M.J., Kirstein, L.,  
1147 2004. Carboniferous-Permian rifting and magmatism in southern Scandinavia, the North Sea and  
1148 northern Germany: a review. *Geological Society, London, Special Publications* 223, 11-40.
- 1149 Nixon, C.W., Sanderson, D.J., Dee, S.J., Bull, J.M., Humphreys, R.J., Swanson, M.H., 2014. Fault  
1150 interactions and reactivation within a normal-fault network at Milne Point, Alaska. *AAPG Bulletin* 98,  
1151 2081-2107.
- 1152 NPD, 2014. Lithostratigraphic chart - Norwegian North Sea,  
1153 . Norwegian Petroleum Directorate (NPD), [https://www.npd.no/globalassets/1-npd/fakta/geologi-  
1154 eng/ns-od1409001.pdf](https://www.npd.no/globalassets/1-npd/fakta/geologi-eng/ns-od1409001.pdf).
- 1155 Odinsen, T., Reemst, P., Beek, P.V.D., Faleide, J.I., Gabrielsen, R.H., 2000. Permo-Triassic and Jurassic  
1156 extension in the northern North Sea: results from tectonostratigraphic forward modelling. *Geological  
1157 Society, London, Special Publications* 167, 83-103.
- 1158 Olsen, H., Briedis, N.A., Renshaw, D., 2017. Sedimentological analysis and reservoir characterization  
1159 of a multi-darcy, billion barrel oil field – The Upper Jurassic shallow marine sandstones of the Johan  
1160 Sverdrup field, North Sea, Norway. *Marine and Petroleum Geology* 84, 102-134.
- 1161 Pascal, C., van Wijk, J.W., Cloetingh, S.A.P.L., Davies, G.R., 2002. Effect of lithosphere thickness  
1162 heterogeneities in controlling rift localization: Numerical modeling of the Oslo Graben. *Geophysical  
1163 Research Letters* 29, 69-61-69-64.
- 1164 Paton, D.A., Mortimer, E.J., Hodgson, N., van der Spuy, D., 2016. The missing piece of the South  
1165 Atlantic jigsaw: when continental break-up ignores crustal heterogeneity. *Geological Society, London,  
1166 Special Publications* 438, SP438.438.
- 1167 Paton, D.A., Underhill, J.R., 2004. Role of crustal anisotropy in modifying the structural and  
1168 sedimentological evolution of extensional basins: the Gamtoos Basin, South Africa. *Basin Res* 16, 339-  
1169 359.
- 1170 Patruno, S., Reid, W., 2016. New plays on the Greater East Shetland Platform (UKCS Quadrants 3, 8-9,  
1171 14-16)–part 1: Regional setting and a working petroleum system. *first break* 34, 33-43.

- 1172 Patruno, S., Reid, W., Berndt, C., Feuillebois, L., 2019. Polyphase tectonic inversion and its role in  
1173 controlling hydrocarbon prospectivity in the Greater East Shetland Platform and Mid North Sea High,  
1174 UK. Geological Society, London, Special Publications 471, 177.
- 1175 Peace, A., McCaffrey, K., Imber, J., van Hunen, J., Hobbs, R., Wilson, R., 2017. The role of pre-existing  
1176 structures during rifting, continental breakup and transform system development, offshore West  
1177 Greenland. *Basin Res*, 373-394.
- 1178 Pegrum, R.M., 1984. The extension of the Tornquist Zone in the Norwegian North Sea. *Norsk*  
1179 *Geologisk Tidsskrift* 64, 39-68.
- 1180 Philippon, M., Willingshofer, E., Sokoutis, D., Corti, G., Sani, F., Bonini, M., Cloetingh, S., 2015. Slip re-  
1181 orientation in oblique rifts. *Geology* 43, 147-150.
- 1182 Phillips, T.B., Jackson, C.A., Bell, R.E., Duffy, O.B., Fossen, H., 2016. Reactivation of intrabasement  
1183 structures during rifting: A case study from offshore southern Norway. *Journal of Structural Geology*  
1184 91, 54-73.
- 1185 Phillips, T.B., Magee, C., Jackson, C.A.L., Bell, R.E., 2017. Determining the three-dimensional  
1186 geometry of a dike swarm and its impact on later rift geometry using seismic reflection data. *Geology*  
1187 46, 119-122.
- 1188 Prosser, S., 1993. Rift-related linked depositional systems and their seismic expression. Geological  
1189 Society, London, Special Publications 71, 35.
- 1190 Quirie, A.K., Schofield, N., Hartley, A., Hole, M.J., Archer, S.G., Underhill, J.R., Watson, D., Holford,  
1191 S.P., 2019. The Rattray Volcanics: Mid-Jurassic fissure volcanism in the UK Central North Sea. *Journal*  
1192 *of the Geological Society* 176, 462-481.
- 1193 Ragon, T., Nutz, A., Schuster, M., Ghienne, J.-F., Ruffet, G., Rubino, J.-L., 2018. Evolution of the  
1194 northern Turkana Depression (East African Rift System, Kenya) during the Cenozoic rifting: New  
1195 insights from the Ekitale Basin (28-25.5 Ma). *Geological Journal* 0.
- 1196 Rattey, R.P., Hayward, A.B., 1993. Sequence stratigraphy of a failed rift system: the Middle Jurassic to  
1197 Early Cretaceous basin evolution of the Central and Northern North Sea. Geological Society, London,  
1198 *Petroleum Geology Conference series* 4, 215-249.
- 1199 Ravnås, R., Bondevik, K., 1997. Architecture and controls on Bathonian–Kimmeridgian shallow-  
1200 marine synrift wedges of the Oseberg–Brage area, northern North Sea. *Basin Res* 9, 197-226.
- 1201 Ravnås, R., Nøttvedt, A., Steel, R.J., Windelstad, J., 2000. Syn-rift sedimentary architectures in the  
1202 Northern North Sea. Geological Society, London, Special Publications 167, 133.
- 1203 Reeve, M.T., Bell, R.E., Duffy, O.B., Jackson, C.A.L., Sansom, E., 2015. The growth of non-colinear  
1204 normal fault systems; What can we learn from 3D seismic reflection data? *Journal of Structural*  
1205 *Geology* 70, 141-155.
- 1206 Reeve, M.T., Bell, R.E., Jackson, C.A.L., 2013. Origin and significance of intra-basement seismic  
1207 reflections offshore western Norway. *Journal of the Geological Society* 171, 1-4.

- 1208 Rey, P., Burg, J.P., Casey, M., 1997. The Scandinavian Caledonides and their relationship to the  
1209 Variscan belt. Geological Society, London, Special Publications 121, 179.
- 1210 Riber, L., Dypvik, H., Sørli, R., 2015. Altered basement rocks on the Utsira High and its surroundings,  
1211 Norwegian North Sea. Norwegian Journal of Geology 95, 57-89.
- 1212 Roberts, A., Yielding, G., Badley, M., 1990. A kinematic model for the orthogonal opening of the late  
1213 Jurassic North Sea rift system, Denmark-Mid Norway. Tectonic Evolution of the North Sea Rifts.  
1214 Clarendon Press, Oxford 180, 199.
- 1215 Roberts, A.M., Yielding, G., Kuszniir, N.J., Walker, I.M., Dorn-Lopez, D., 1995. Quantitative analysis of  
1216 Triassic extension in the northern Viking Graben. Journal of the Geological Society 152, 15.
- 1217 Roberts, D., 2003. The Scandinavian Caledonides: event chronology, palaeogeographic settings and  
1218 likely modern analogues. Tectonophysics 365, 283-299.
- 1219 Roberts, D.G., Thompson, M., Mitchener, B., Hossack, J., Carmichael, S., Bjørnseth, H.M., 1999.  
1220 Palaeozoic to Tertiary rift and basin dynamics: mid-Norway to the Bay of Biscay – a new context for  
1221 hydrocarbon prospectivity in the deep water frontier. Geological Society, London, Petroleum Geology  
1222 Conference series 5, 7.
- 1223 Roffeis, C., Corfu, F., 2013. Caledonian nappes of southern Norway and their correlation with  
1224 Sveconorwegian basement domains. Geological Society, London, Special Publications 390, 193-221.
- 1225 Rotevatn, A., Kristensen, T.B., Ksienzyk, A.K., Wemmer, K., Henstra, G.A., Midtkandal, I., Grundvåg, S.-  
1226 A., Andresen, A., 2018. Structural Inheritance and Rapid Rift-Length Establishment in a Multiphase  
1227 Rift: The East Greenland Rift System and its Caledonian Orogenic Ancestry. Tectonics 37, 1858-1875.
- 1228 Salomon, E., Koehn, D., Passchier, C., 2015. Brittle reactivation of ductile shear zones in NW Namibia  
1229 in relation to South Atlantic rifting. Tectonics 34, 70-85.
- 1230 Samsu, A., Cruden, A.R., Hall, M., Micklethwaite, S., Denyszyn, S.W., 2019. The influence of basement  
1231 faults on local extension directions: Insights from potential field geophysics and field observations.  
1232 Basin Res 0.
- 1233 Scisciani, V., Patruno, S., Tavarnelli, E., Calamita, F., Pace, P., Iacopini, D., 2019. Multi-phase  
1234 reactivations and inversions of Paleozoic-Mesozoic extensional basins during the Wilson Cycle: case  
1235 studies from the North Sea (UK) and Northern Apennines (Italy). Geological Society, London, Special  
1236 Publications 470, SP470-2017-2232.
- 1237 Seranne, M., Seguret, M., 1987. The Devonian basins of western Norway: tectonics and kinematics of  
1238 an extending crust. Geological Society, London, Special Publications 28, 537-548.
- 1239 Skyttä, P., Piippo, S., Kloppenburg, A., Corti, G., 2019. 2. 45 Ga break-up of the Archaean continent in  
1240 Northern Fennoscandia: Rifting dynamics and the role of inherited structures within the Archaean  
1241 basement. Precambrian Research.

- 1242 Slagstad, T., Davidsen, B., Daly, J.S., 2011. Age and composition of crystalline basement rocks on the  
1243 Norwegian continental margin: offshore extension and continuity of the Caledonian–Appalachian  
1244 orogenic belt. *Journal of the Geological Society* 168, 1167.
- 1245 Slagstad, T., Roberts, N.M.W., Marker, M., Røhr, T.S., Schiellerup, H., 2013. A non-collisional,  
1246 accretionary Sveconorwegian orogen. *Terra Nova* 25, 30-37.
- 1247 Smethurst, M.A., 2000. Land–offshore tectonic links in western Norway and the northern North Sea.  
1248 *Journal of the Geological Society* 157, 769-781.
- 1249 Sømme, T.O., Lunt, I., Martinsen, O.J., 2013. Linking offshore stratigraphy to onshore  
1250 paleotopography: The Late Jurassic–Paleocene evolution of the south Norwegian margin. *GSA*  
1251 *Bulletin* 125, 1164-1186.
- 1252 Sorento, T., Stemmerik, L., Olausson, S., 2018. Upper Permian carbonates at the northern edge of the  
1253 Zechstein basin, Utsira High, Norwegian North Sea. *Marine and Petroleum Geology* 89, 635-652.
- 1254 Steltenpohl, M.G., Hames, W.E., Andresen, A., 2004. The Silurian to Permian history of a  
1255 metamorphic core complex in Lofoten, northern Scandinavian Caledonides. *Tectonics* 23.
- 1256 Stewart, I.J., Rattey, R.P., Vann, I.R., 1992. Structural style and the habitat of hydrocarbons in the  
1257 North Sea, in: Larsen, R.M., Brekke, H., Larsen, B.T., Talleraas, E. (Eds.), *Structural and Tectonic*  
1258 *Modelling and its Application to Petroleum Geology*. Elsevier, Amsterdam, pp. 197-220.
- 1259 Stewart, S., Ries, A., Butler, R., Graham, R., 2007. Salt tectonics in the North Sea Basin: a structural  
1260 style template for seismic interpreters. *Special Publication-Geological Society of London* 272, 361.
- 1261 Stewart, S.A., Coward, M.P., 1995. Synthesis of salt tectonics in the southern North Sea, UK. *Marine*  
1262 *and Petroleum Geology* 12, 457-475.
- 1263 Ter Voorde, M., Færseth, R.B., Gabrielsen, R.H., Cloetingh, S.A.P.L., 2000. Repeated lithosphere  
1264 extension in the northern Viking Graben: a coupled or a decoupled rheology? *Geological Society,*  
1265 *London, Special Publications* 167, 59.
- 1266 Thon, A., 1980. Steep shear zones in the basement and associated deformation of the cover  
1267 sequence on Karmøy, SW Norwegian Caledonides. *Journal of Structural Geology* 2, 75-80.
- 1268 Tomasso, M., Underhill, J.R., Hodgkinson, R.A., Young, M.J., 2008. Structural styles and depositional  
1269 architecture in the Triassic of the Ninian and Alwyn North fields: Implications for basin development  
1270 and prospectivity in the Northern North Sea. *Marine and Petroleum Geology* 25, 588-605.
- 1271 Tong, H., Yin, A., 2011. Reactivation tendency analysis: A theory for predicting the temporal evolution  
1272 of preexisting weakness under uniform stress state. *Tectonophysics* 503, 195-200.
- 1273 Underhill, J.R., Partington, M.A., 1993. Jurassic thermal doming and deflation in the North Sea:  
1274 implications of the sequence stratigraphic evidence. 337-345.

- 1275 Vasconcelos, D.L., Bezerra, F.H.R., Medeiros, W.E., de Castro, D.L., Clausen, O.R., Vital, H., Oliveira,  
1276 R.G., 2019. Basement fabric controls rift nucleation and postrift basin inversion in the continental  
1277 margin of NE Brazil. *Tectonophysics* 751, 23-40.
- 1278 Vetti, V.V., Fossen, H., 2012. Origin of contrasting Devonian supradetachment basin types in the  
1279 Scandinavian Caledonides. *Geology* 40, 571-574.
- 1280 Wenker, S., Beaumont, C., 2016. Effects of lateral strength contrasts and inherited heterogeneities on  
1281 necking and rifting of continents. *Tectonophysics*.
- 1282 Whipp, P.S., Jackson, C.A.L., Gawthorpe, R.L., Dreyer, T., Quinn, D., 2014. Normal fault array  
1283 evolution above a reactivated rift fabric; a subsurface example from the northern Horda Platform,  
1284 Norwegian North Sea. *Basin Res* 26, 523-549.
- 1285 Wiest, J.D., Jacobs, J., Ksienzyk, A.K., Fossen, H., 2018. Sveconorwegian vs. Caledonian orogenesis in  
1286 the eastern Øygarden Complex, SW Norway – Geochronology, structural constraints and tectonic  
1287 implications. *Precambrian Research* 305, 1-18.
- 1288 Wilson, M., Neumann, E.-R., Davies, G.R., Timmerman, M., Heeremans, M., Larsen, B.T., 2004.  
1289 Permo-Carboniferous magmatism and rifting in Europe: introduction. Geological Society, London,  
1290 Special Publications 223, 1-10.
- 1291 Youash, Y., 1969. Tension Tests on Layered Rocks. *Geological Society of America Bulletin* 80, 303-306.
- 1292 Zang, A., Stephansson, O., 2009. Stress field of the Earth's crust. Springer Science & Business Media.
- 1293 Ziegler, P.A., 1992. North-Sea Rift System. *Tectonophysics* 208, 55-75.
- 1294

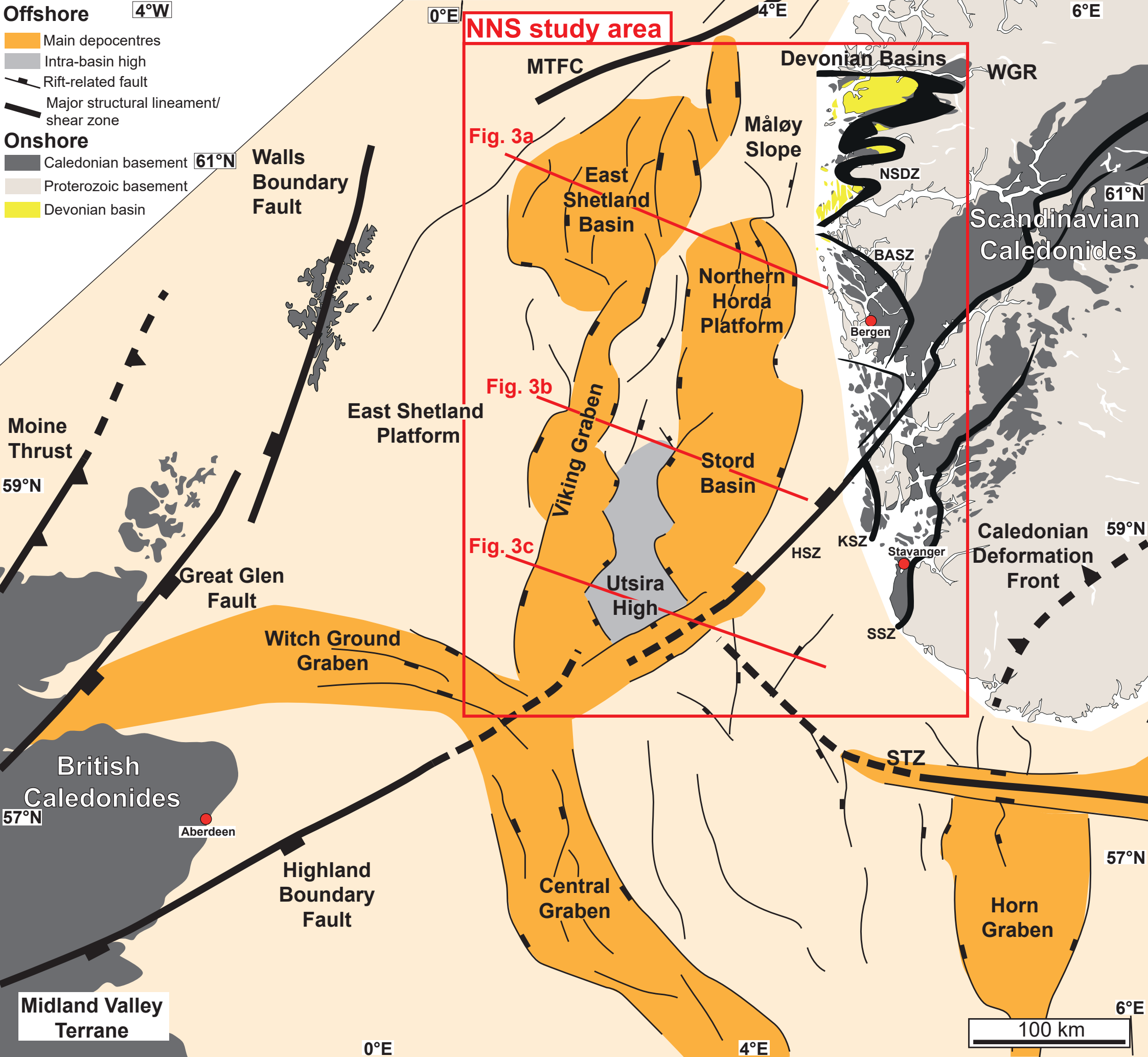
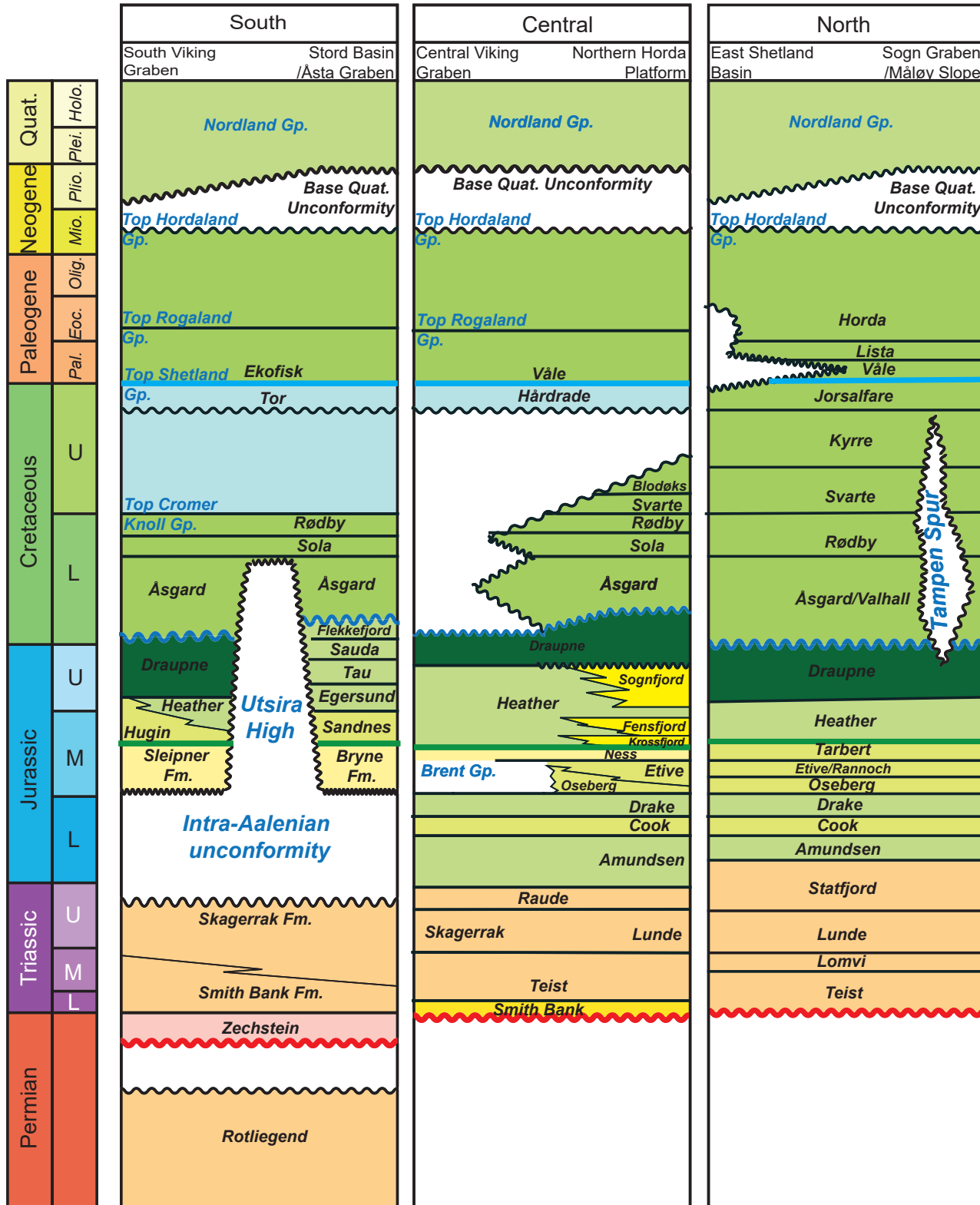


Figure 1

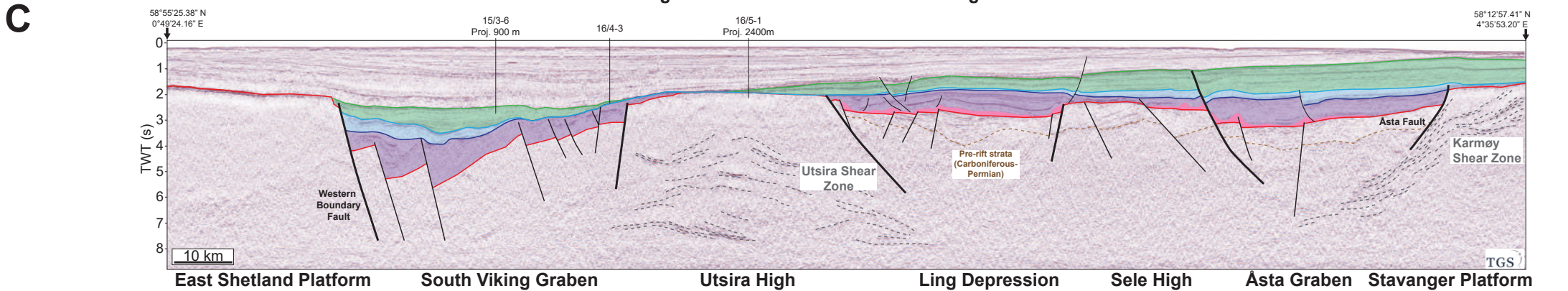
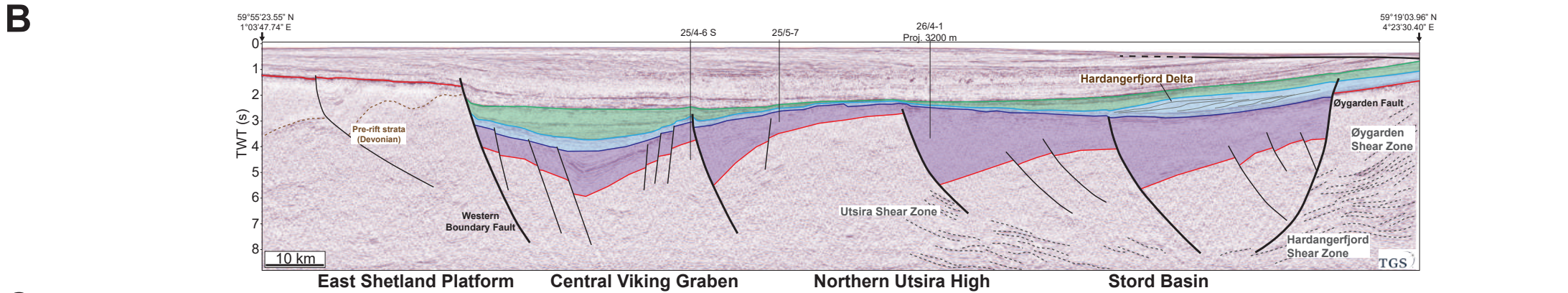
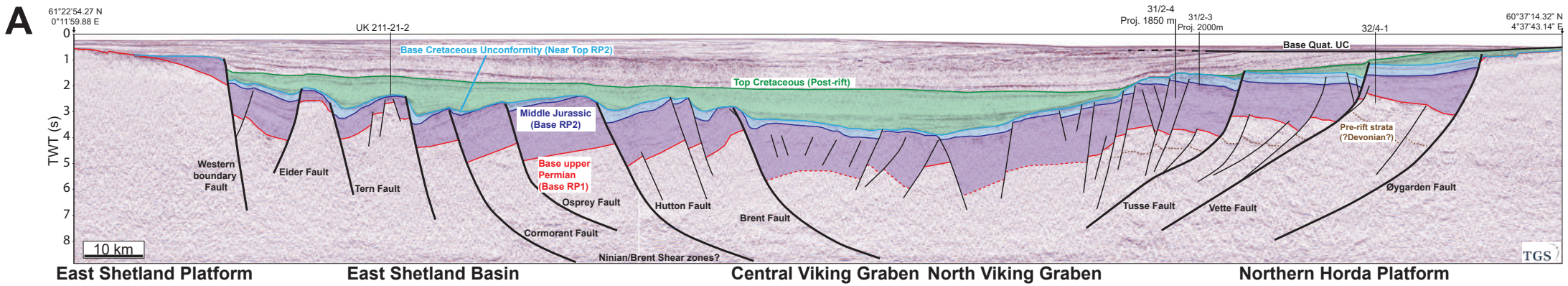


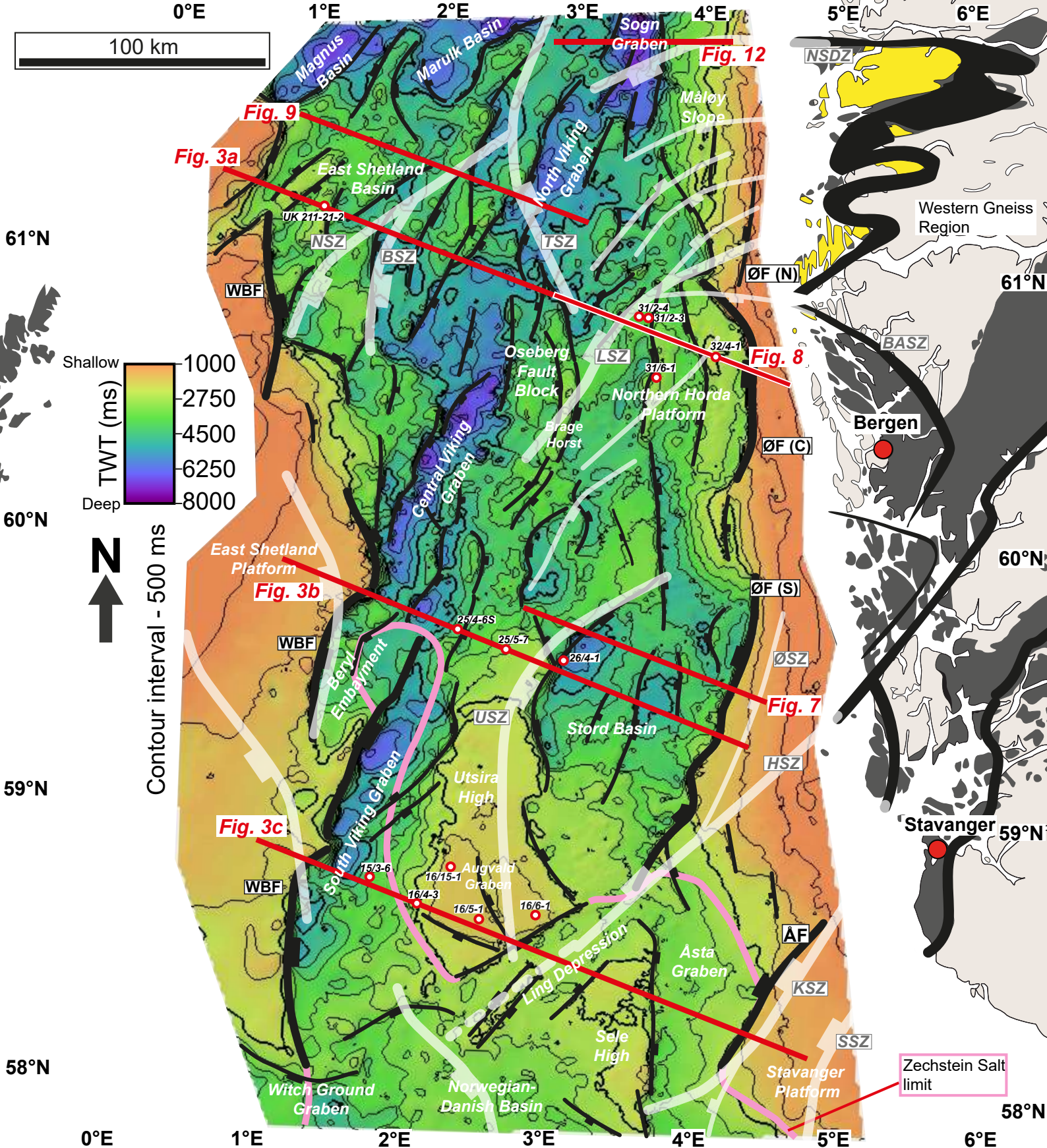
Top Cretaceous Post-rift

BCU Near Top RP2

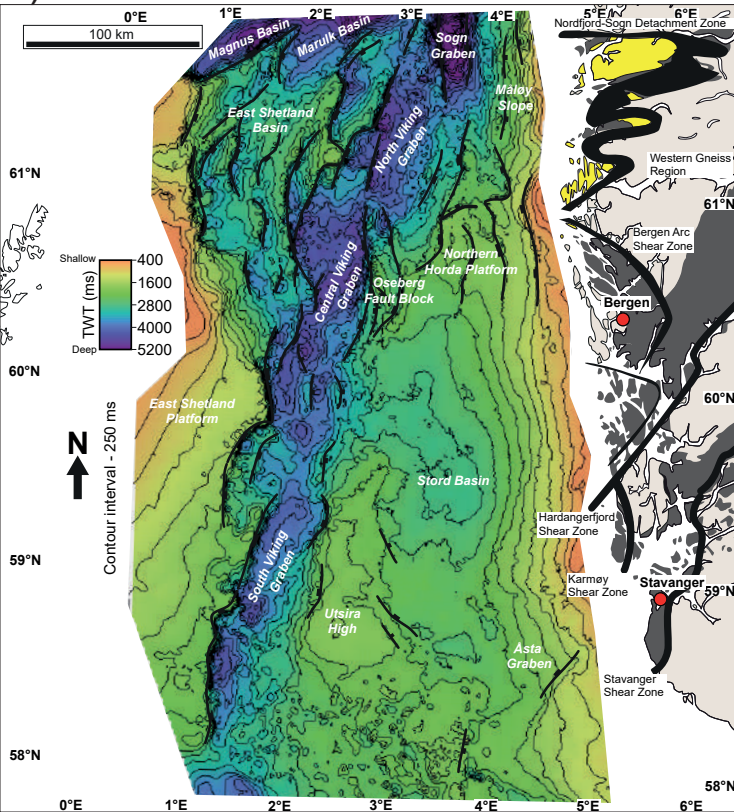
Middle Jurassic Base RP2

Base RP1

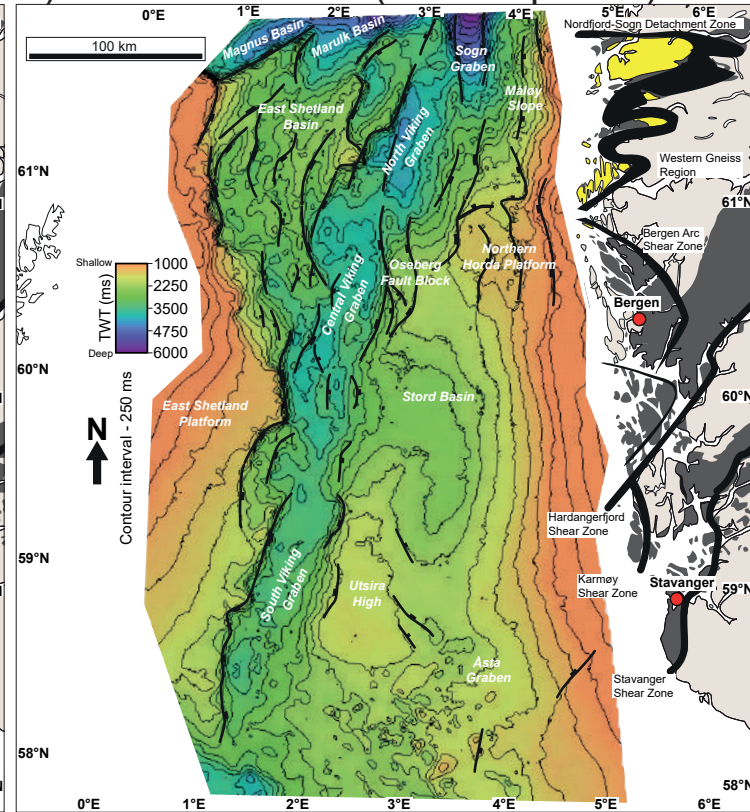




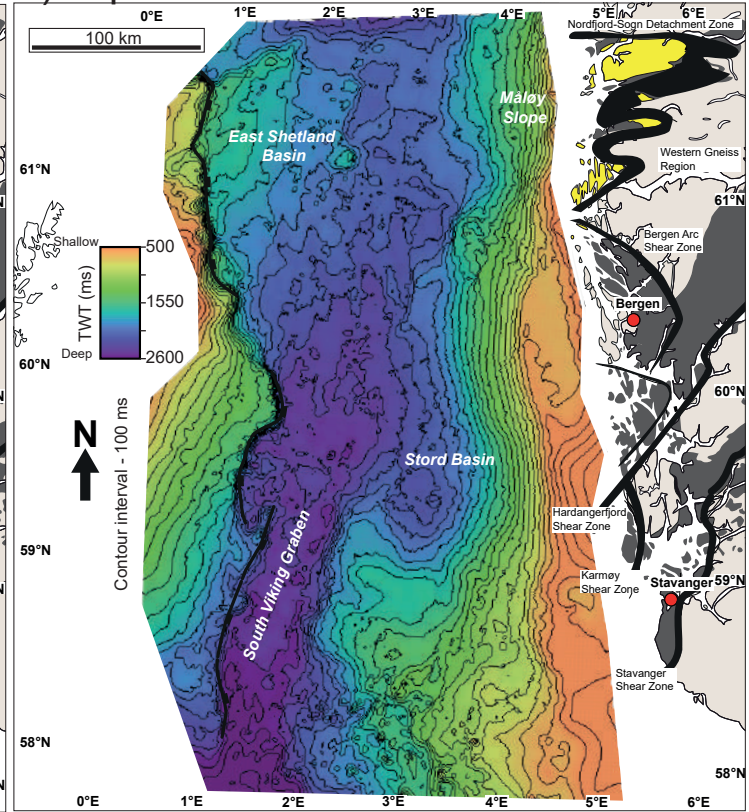
A) Middle Jurassic - Base RP2

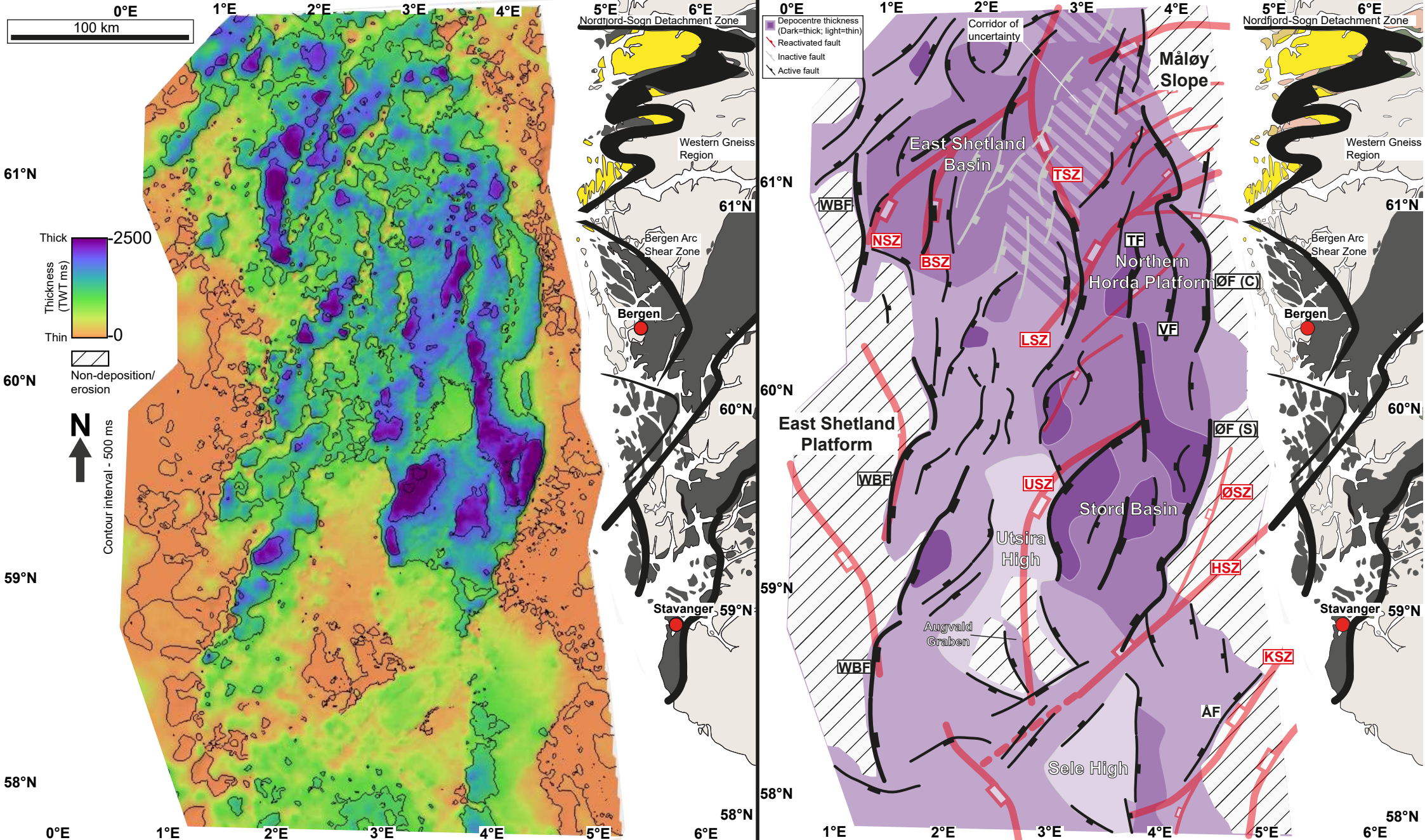


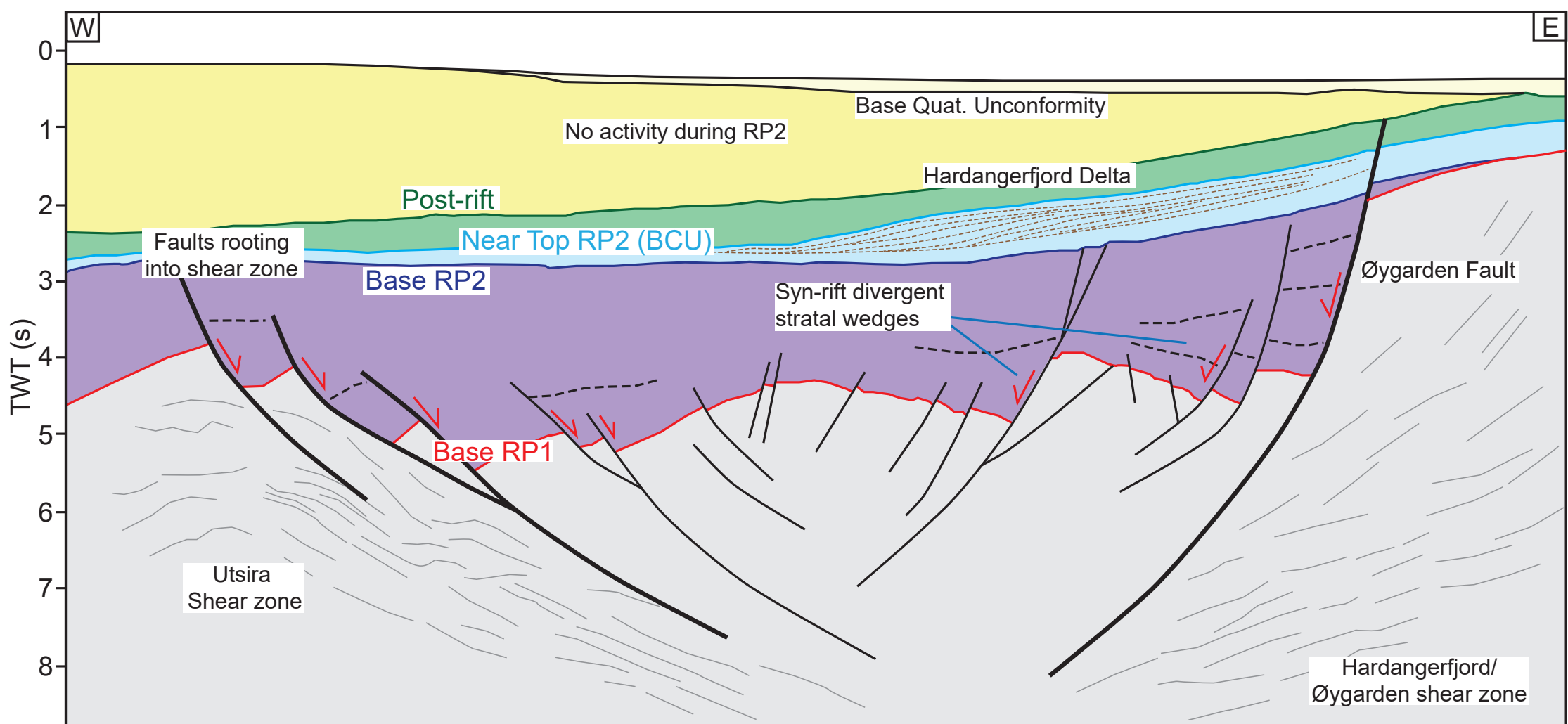
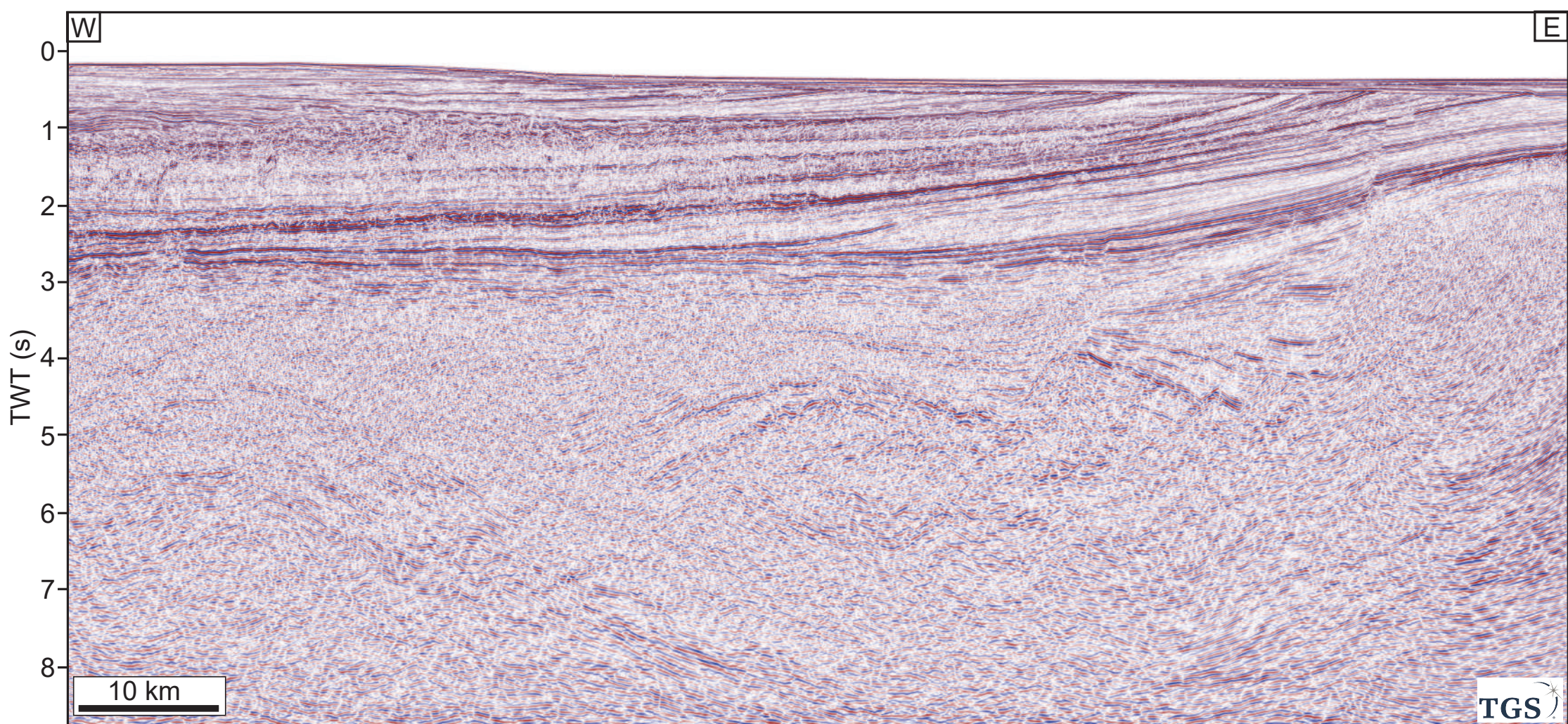
B) Base Cret. Unc. (Near Top RP2)

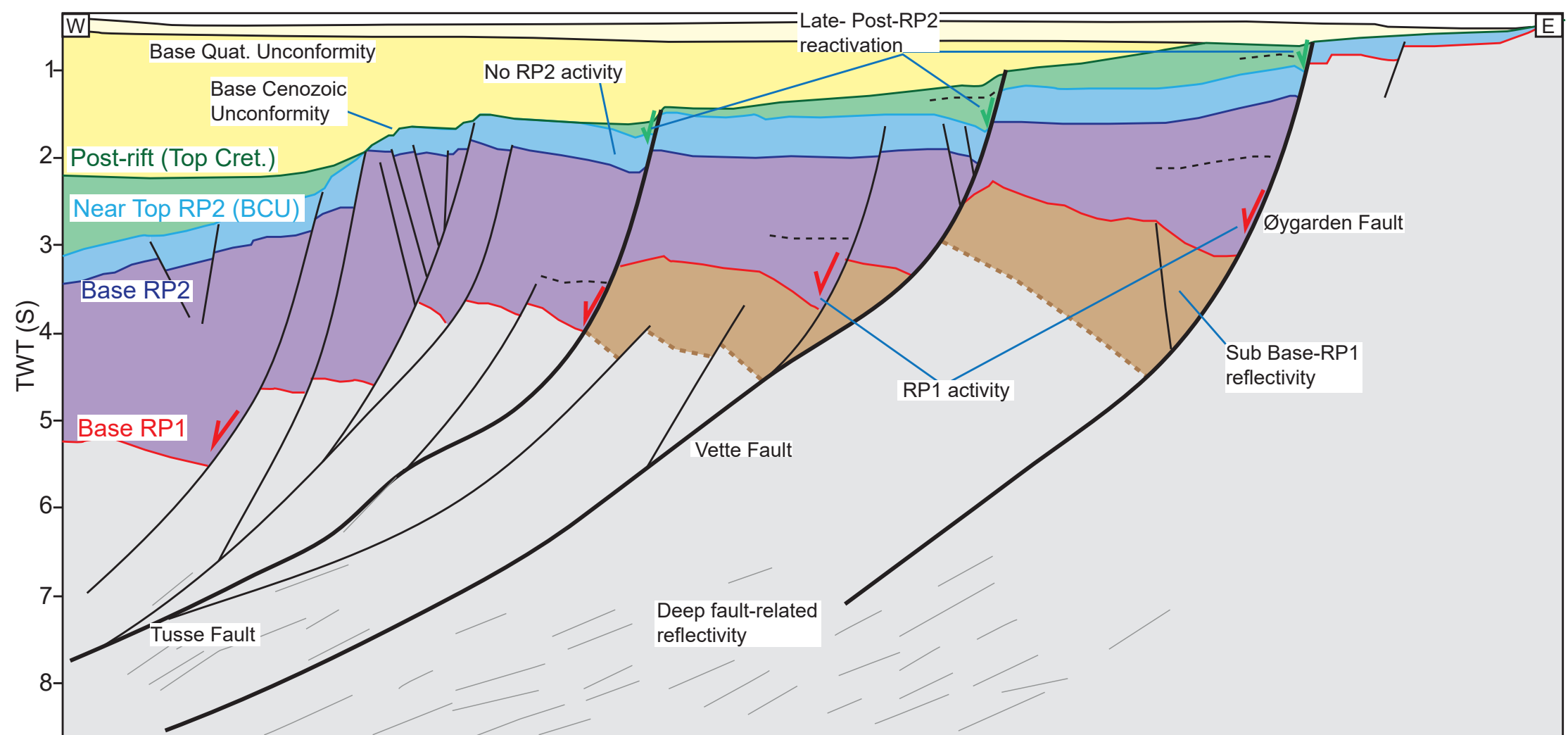
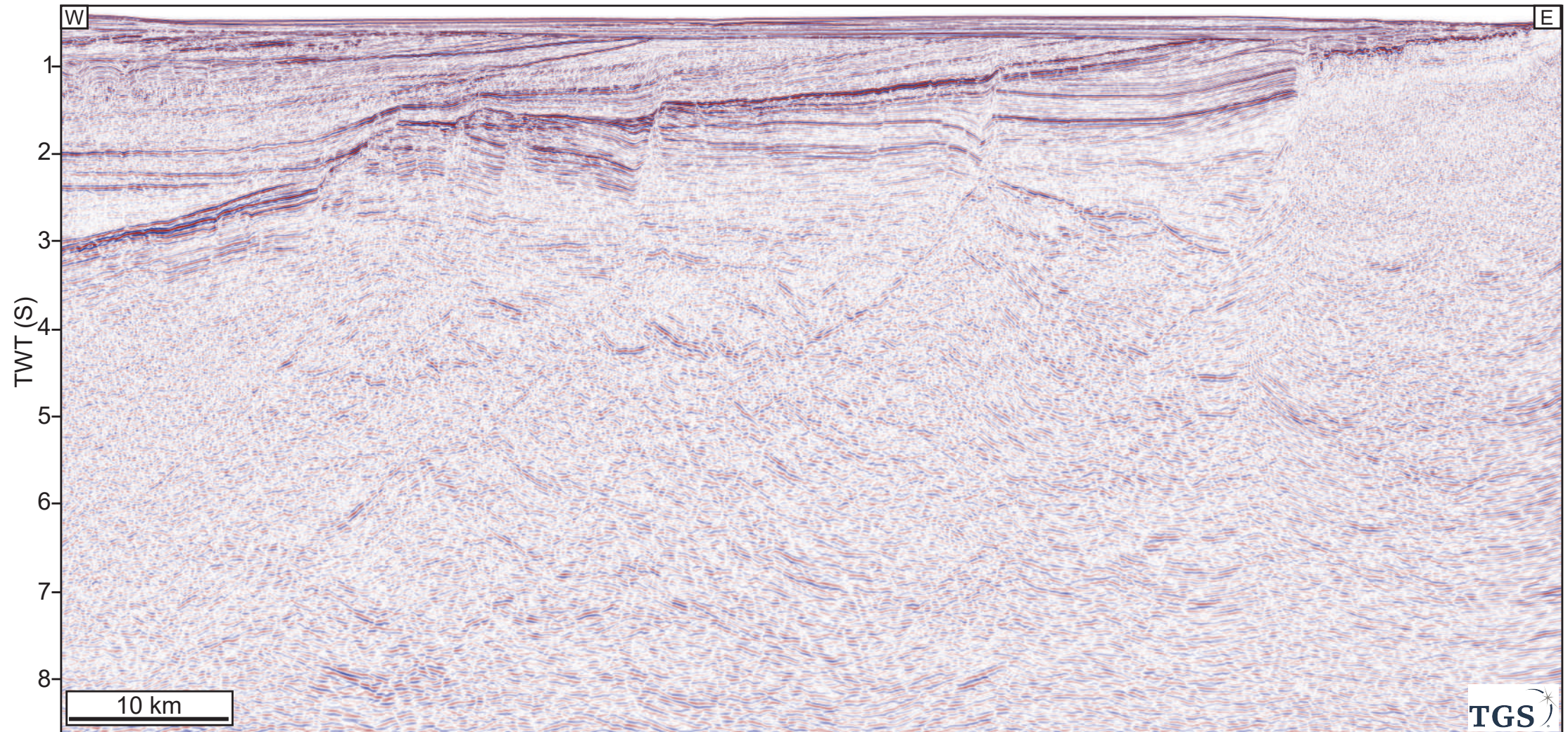


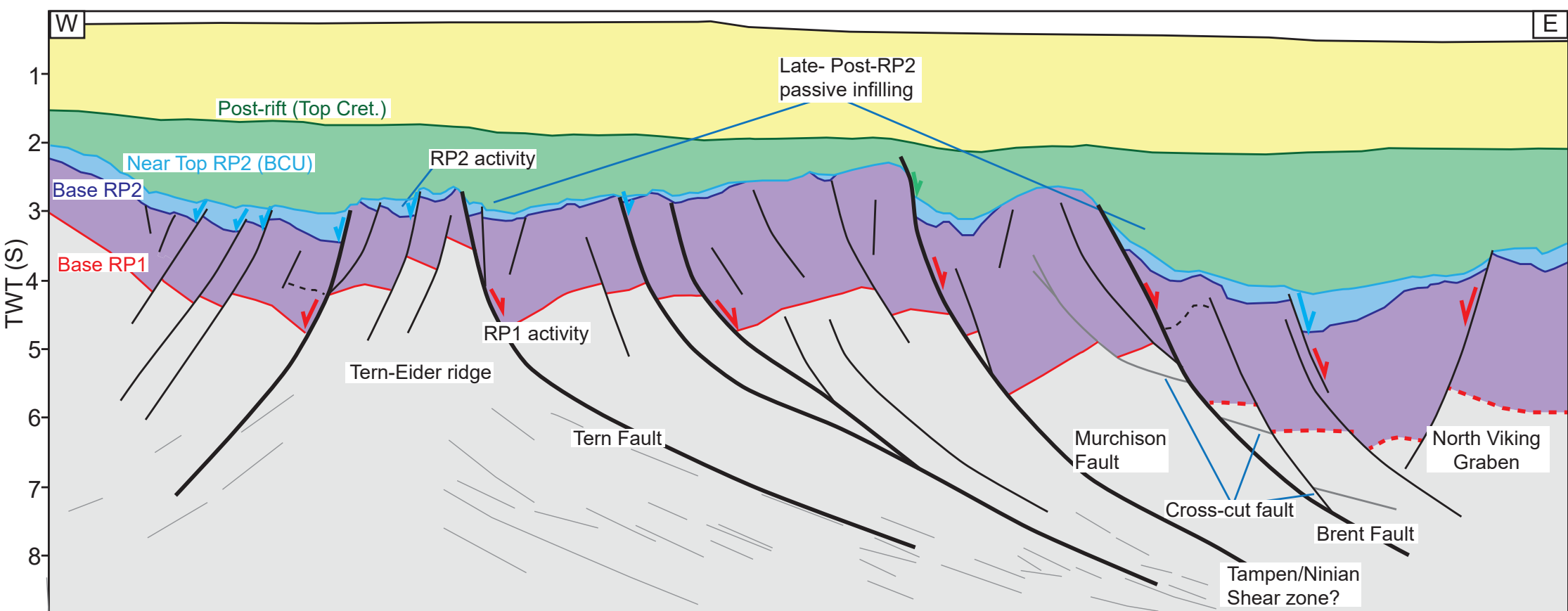
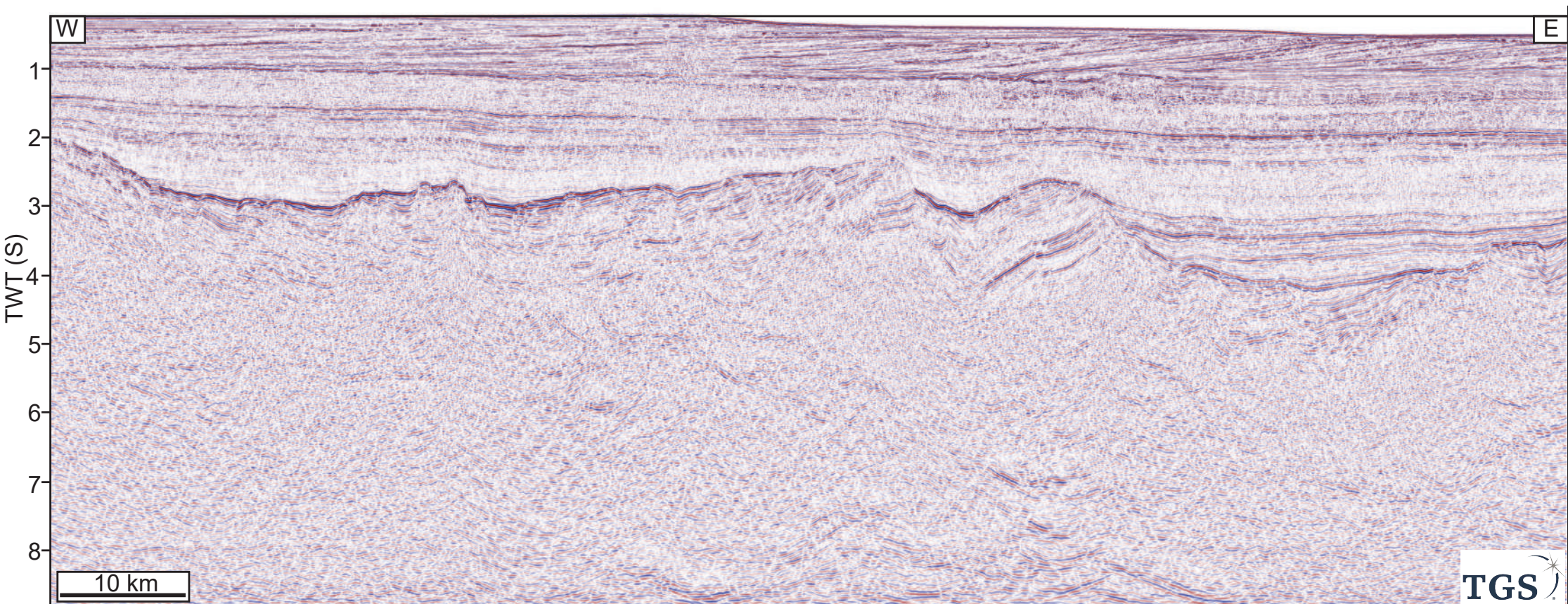
C) Top Cretaceous - Post-rift

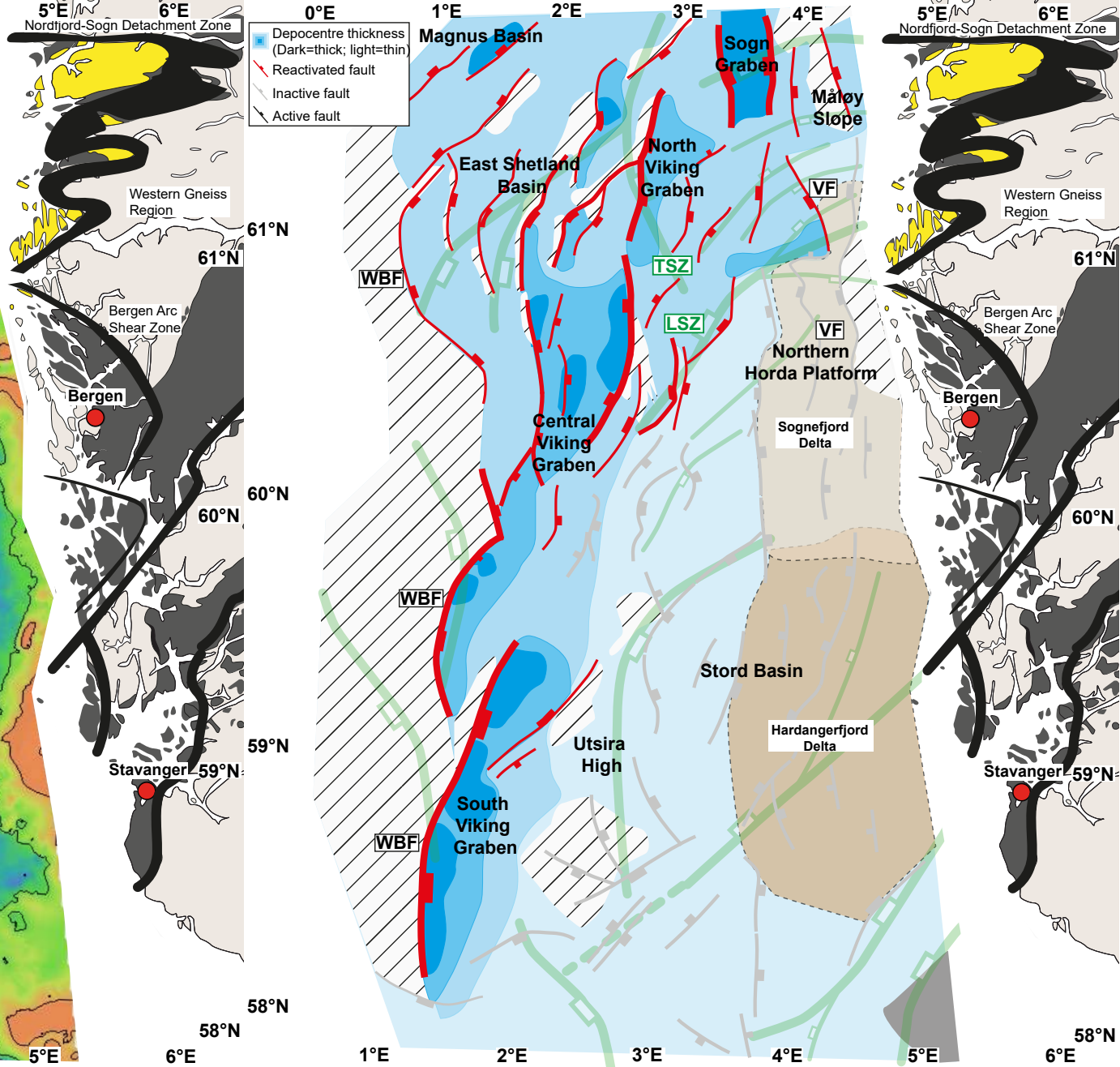
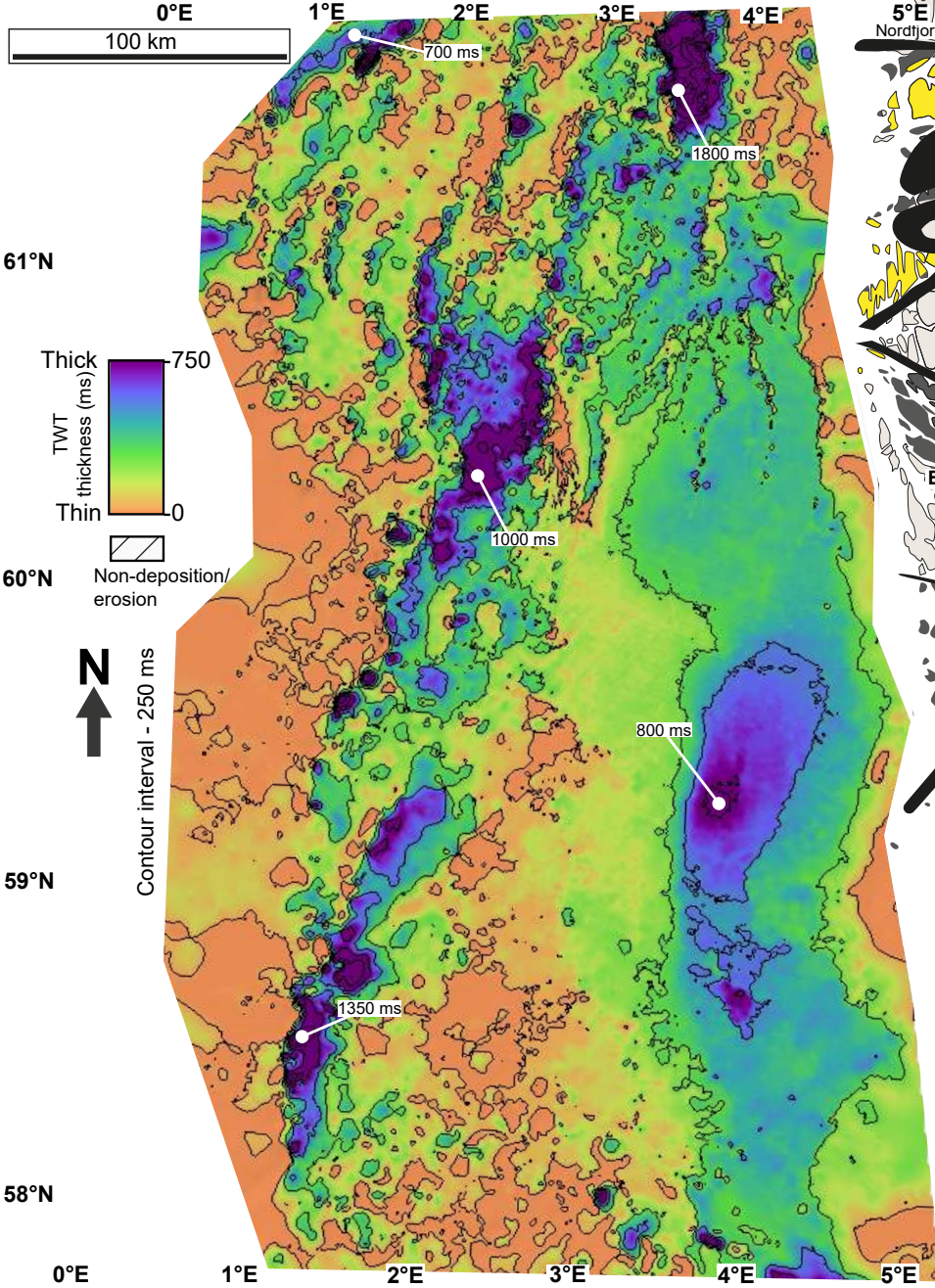


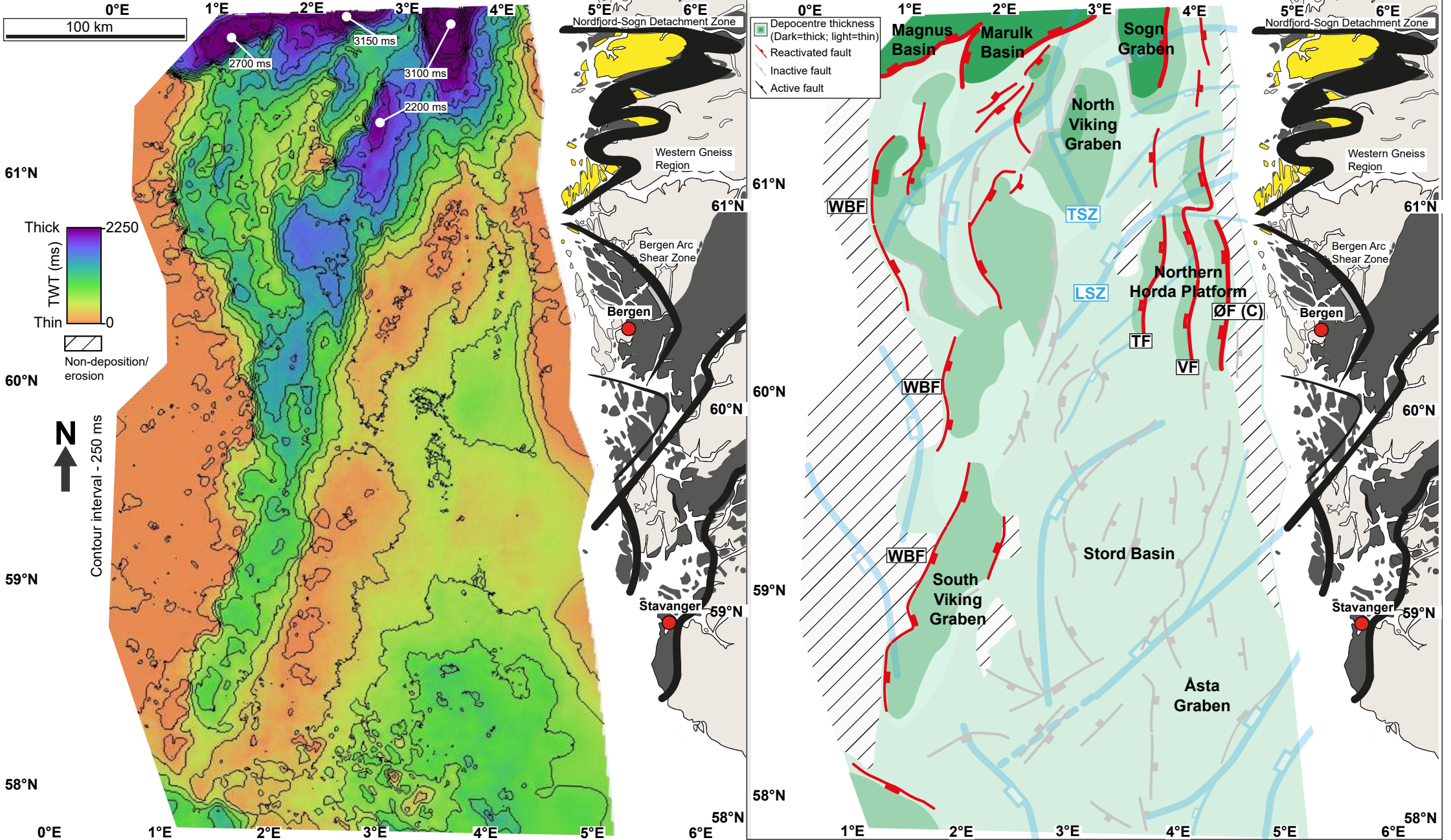


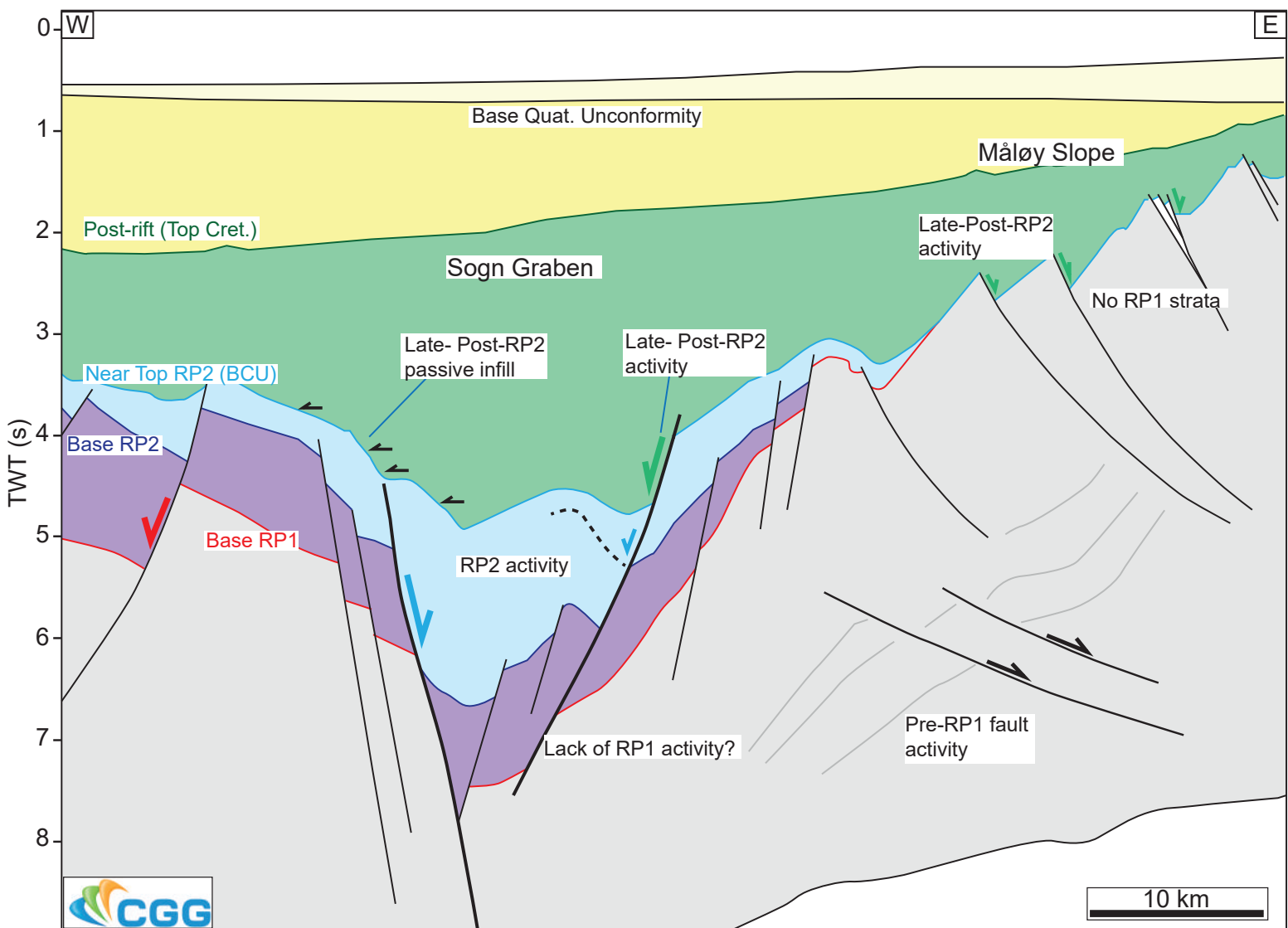
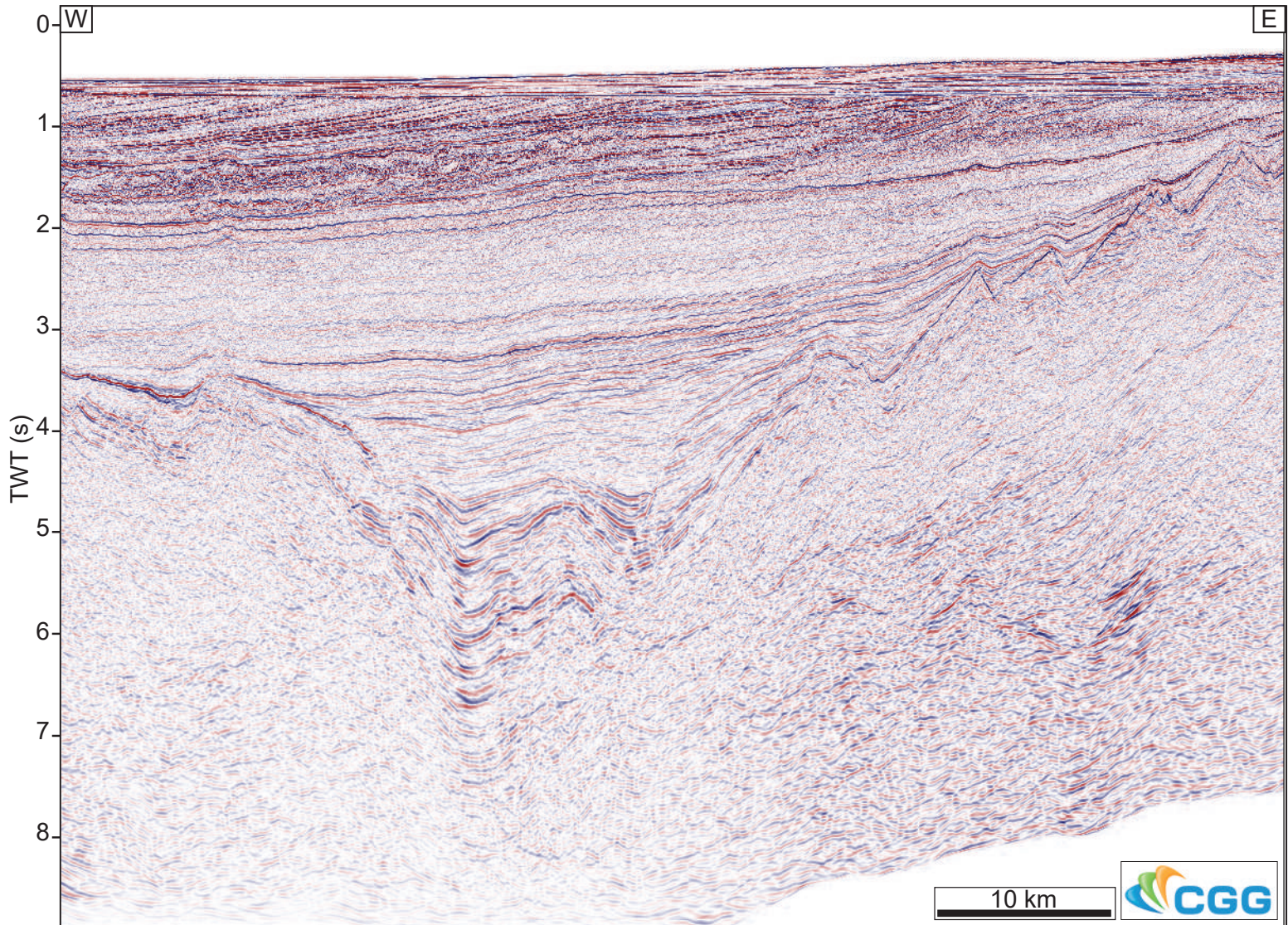




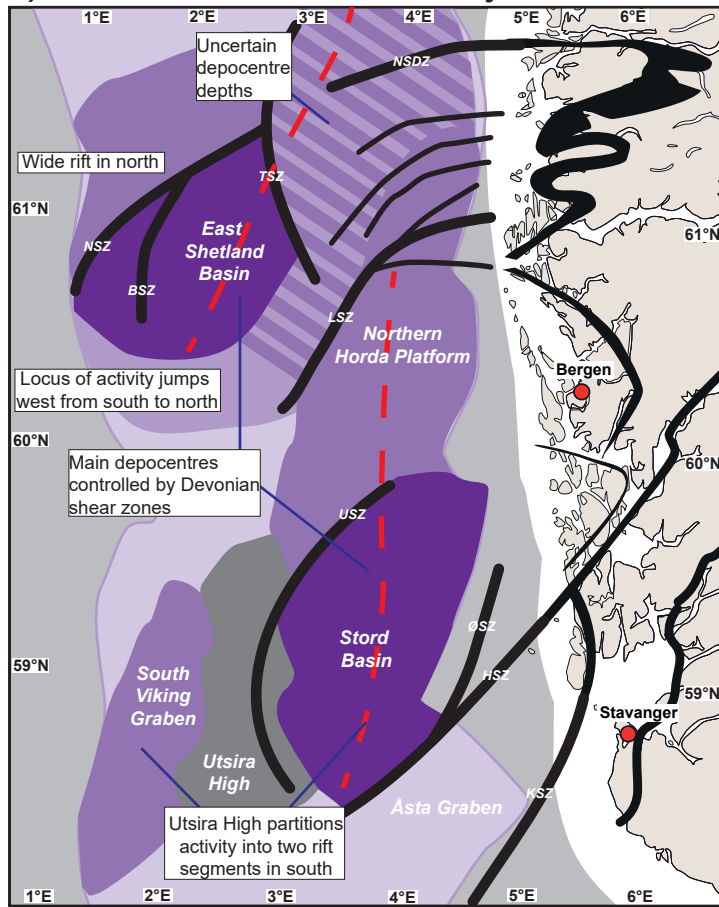




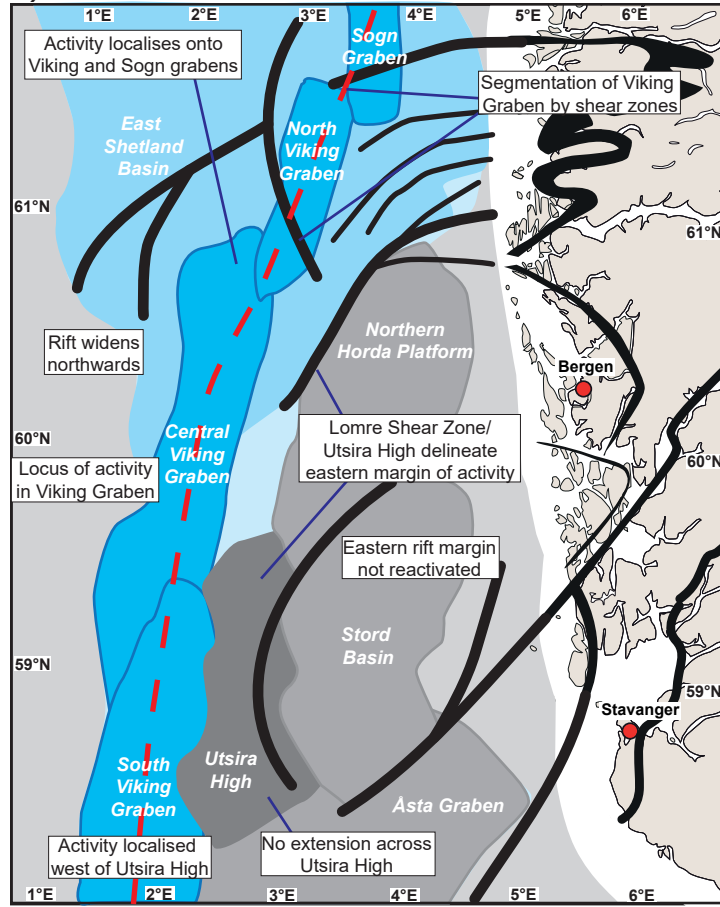




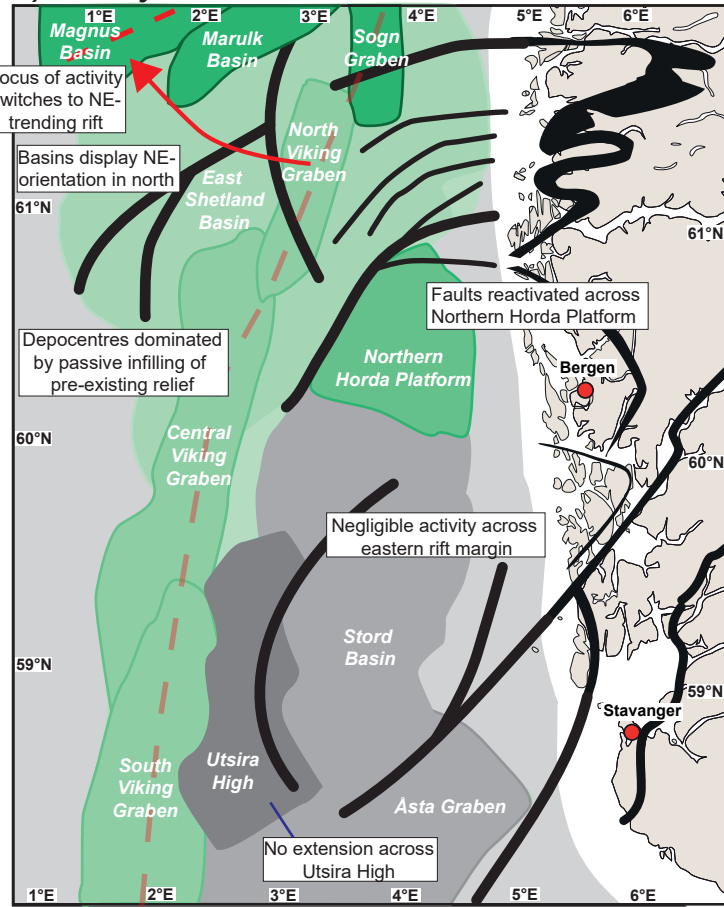
### A) Rift Phase 1 - late Permian-Early Triassic

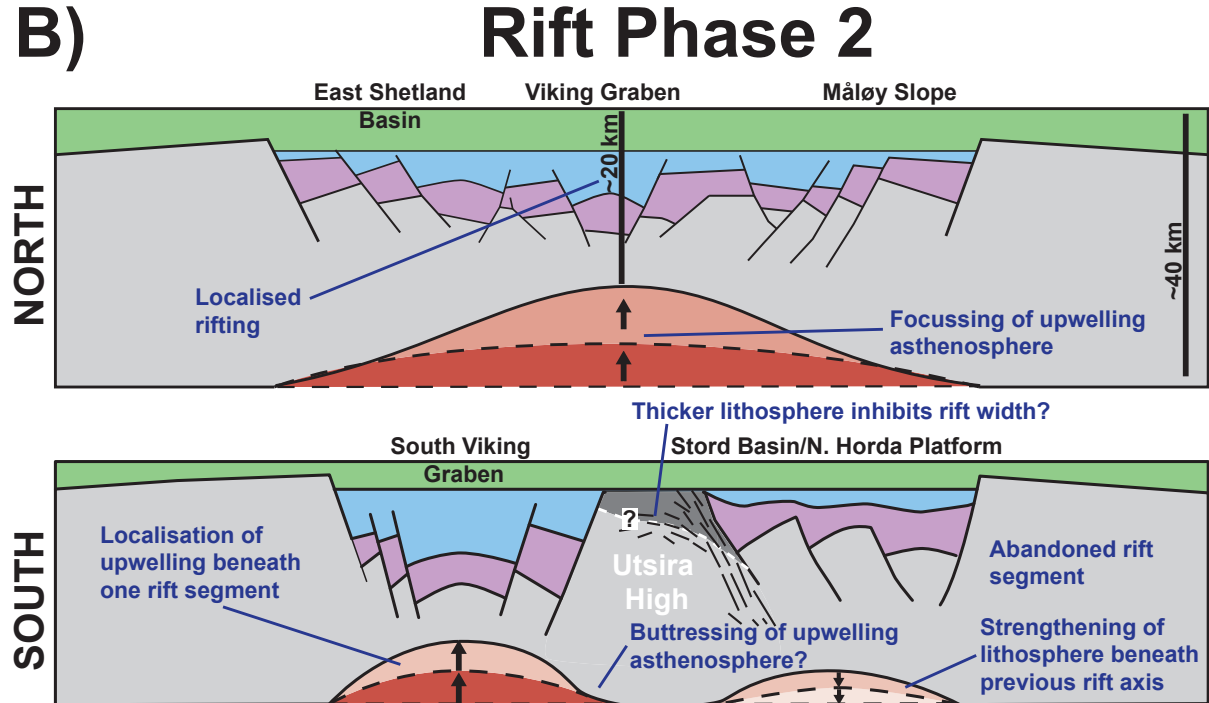
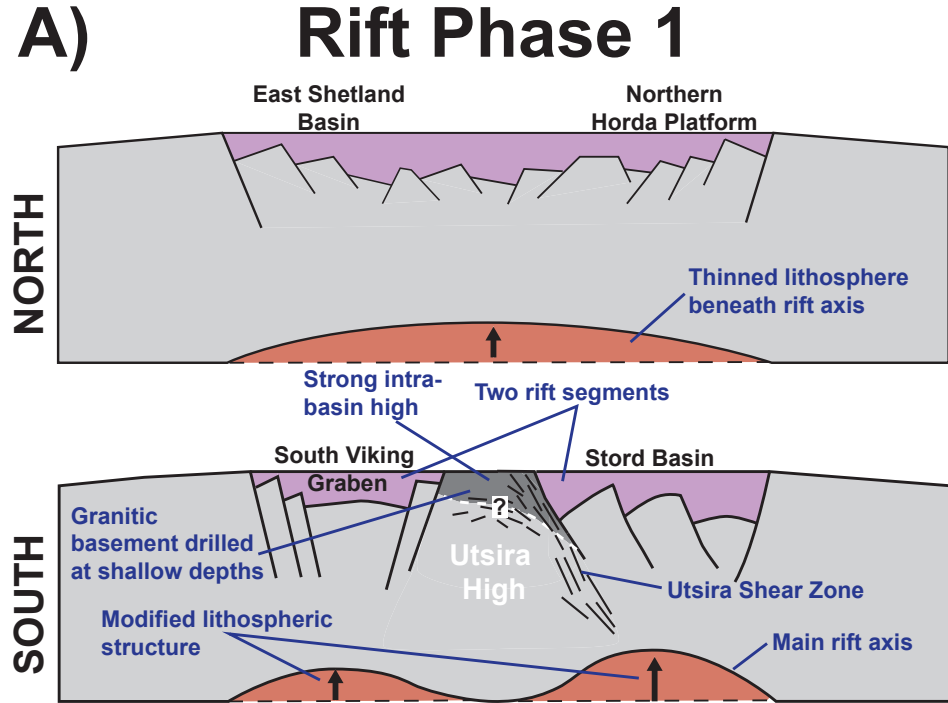


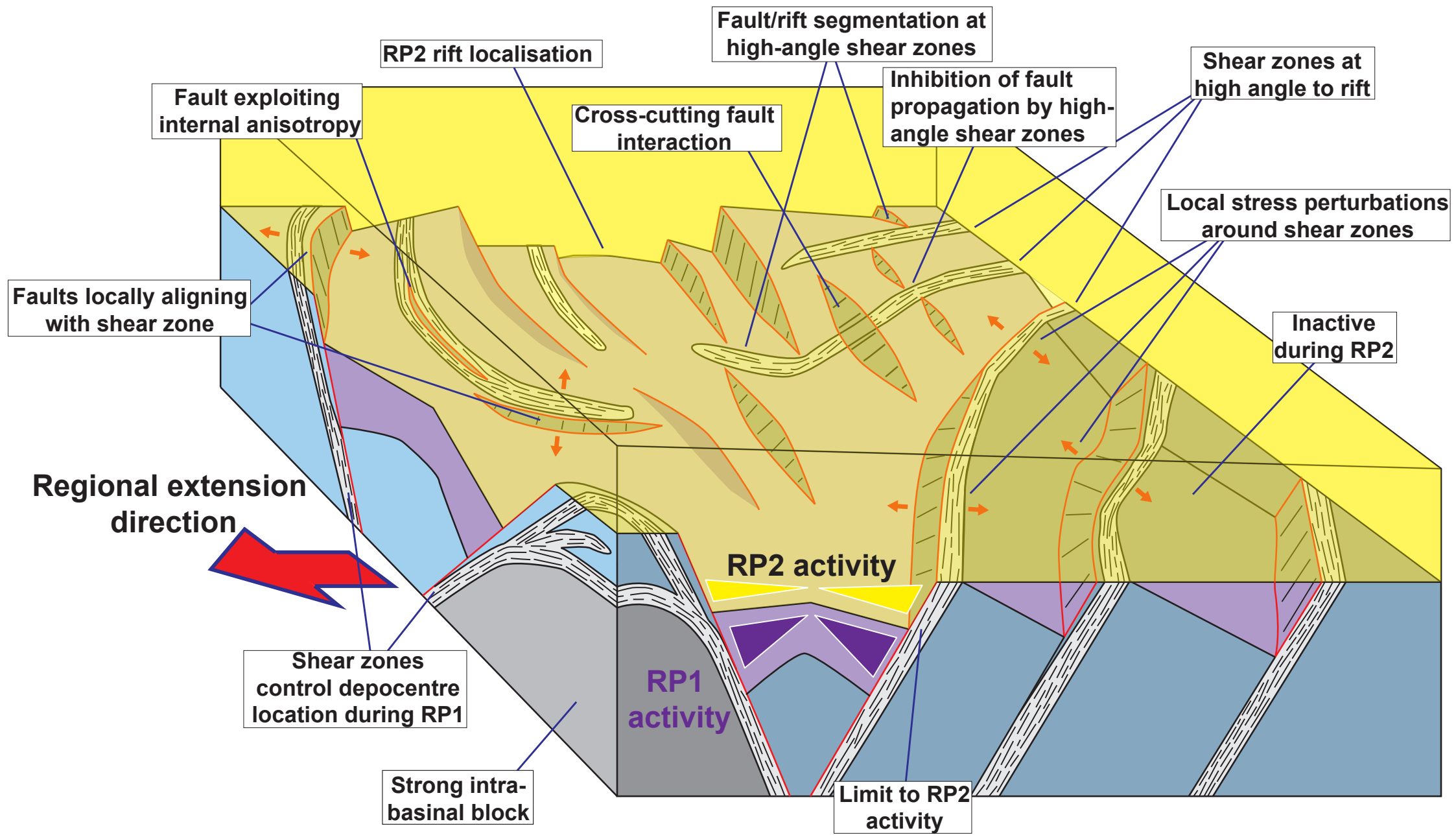
### B) Rift Phase 2 - Middle Jurassic-BCU



### C) Late-syn- to Post-Rift Phase 2 - Cretaceous







*Tectonics*

Supporting Information for

**The influence of structural inheritance and multiphase extension on rift development, the northern North Sea**

Thomas B. Phillips<sup>1,2</sup>; Hamed Fazlikhani<sup>2†</sup>; Rob L. Gawthorpe<sup>2</sup>; Haakon Fossen<sup>2,3</sup>; Christopher A-L. Jackson<sup>4</sup>; Rebecca E. Bell<sup>4</sup>; Jan I. Faleide<sup>5</sup>; Atle Rotevatn<sup>4</sup>

<sup>1</sup>Department of Earth Sciences, Durham University, Science Labs, Elvet Hill, Durham, DH1 3LE

<sup>2</sup> Department of Earth Science, University of Bergen, PO Box 7800, 5020 Bergen, Norway

<sup>3</sup> Natural History Collections, University of Bergen, PO Box 7800, 5020 Bergen, Norway

<sup>4</sup>Basins Research Group (BRG), Department of Earth Science and Engineering, Imperial College, Prince Consort Road, London SW7 2BP, UK

<sup>5</sup>Department of Geosciences, University of Oslo, PO Box 1047, 0316 Oslo, Norway

<sup>†</sup>Present address: GeoZentrum Nordbayern, Friedrich-Alexander-Universität (FAU) Erlangen-Nürnberg, Schlossgarten 5, 91054 Erlangen, Germany

## **Contents of this file**

Figure S1

Tables S1 to S2

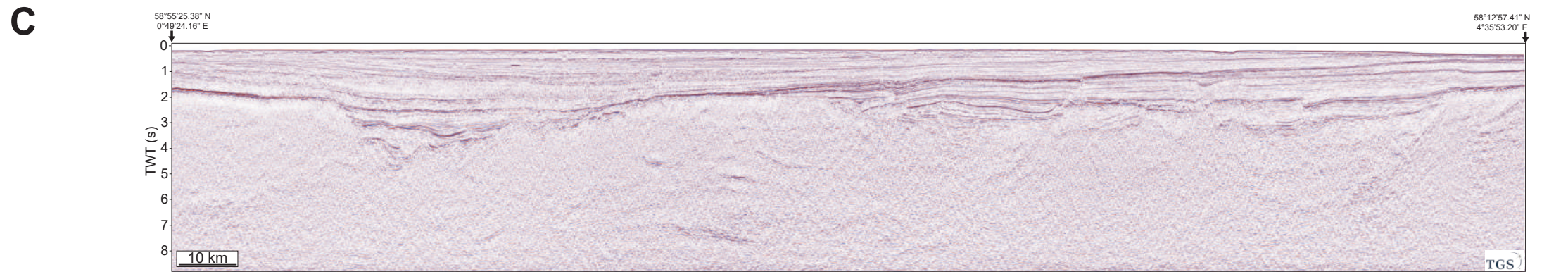
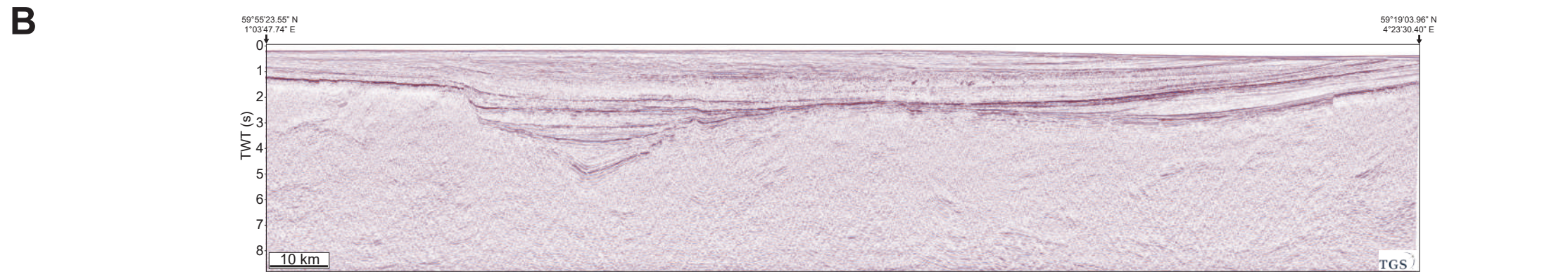
## **Introduction**

This supporting information contains uninterpreted versions of the seismic sections shown in Figure 3, as well as summary tables detailing the acquisition and processing parameters of the seismic surveys used in this study (Table S1) and the basement penetrating wells in the study area (Table S2)

**Figure S1.** Uninterpreted seismic sections of Figure 3.

**Table S1.** Summary of seismic surveys and their acquisition parameters as used in this study. From Fazlikhani et al. (2017).

**Table S2.** Table showing basement penetrating exploration wells used in this study, after Fazlikhani et al. (2017). Depths shown are measured depth (MD) from the Kelly Bushing (KB) datum. Well information shown by asterisk is from Bassett (2003) and Marshall & Hewett (2003).



Seismic survey	Acquisition date	Length (km)	Source interval (m)	Streamer length \separation (m)	Sample interval (ms)	Record length (s)
CNST-86	1986	5,764	25	3000	4	7
CNSTE-N-83	1983	800	25	3000	4	7
EL-9202	1992	307	25	-	4	6
GLD-92	1992	1,287	25	-	4	7
GNSR-91	1991	11,322	25	-	4	9
GSB-85	1985	4,082	25	-	4	7
HPS-98	1998	2,643	25	-	4	6
HRT-93	1993	1,390	25	-	4	7
HT-91	1991	224	25	-	4	7
NNST-84	1984	8,099	25	3000	2	7
NNSTI-86	1986	684	25	3000	2	7
NNSTI-87	1987	613	25	3000	2	7
NSDP-84	1984	1,689	25	-	4	15
NSR-03-12	2003-12	244,417	25	1x7950\8100	2	9.2
NVGT-88	1988	3,611	25	-	4	7
NVGTI-92	1992	3,158	25	-	4	7
SBGS-94RE	1994	2,584	25	-	4	7
SG-8043	1980	545	25	-	4	7
SG-8146	1981	2,063	25	-	4	7
SG-9009	1990	567	25	-	4	7
SG-9617	1996	1,273	25	-	4	7
SH-8001	1980	3,950	25	-	4	5
ST-8107WE	1981	166	25	-	4	5
ST-8201-8301	1982-83	6,182	25	-	4	6
ST-8408	1984	4,261	25	-	4	7
ST-8503	1985	2,761	25	-	4	7
ST-8620	1986	704	25	-	4	7
ST-8703	1987	75	25	-	4	7
TE-90	1990	1,814	25	-	4	6

**Table S1.** - Summary of seismic surveys and their acquisition parameters as used in this study. From Fazlikhani et al. (2017).

Well name	Top basement (MD,KB), m	Drilled thickness (m)	Basement rock types	Interpretation
8,3-1	2965	50	Schist	Caledonian allochthon
15,5-3	4850	200	Shale, siltstone and sandstone	Devonian
16,1-2	2912	25	Granite- Pink	Caledonian allochthon
16,1-3	3440	57	Granite	Caledonian allochthon
16,1-4	1864	146	Hornblende-gabbro	Caledonian allochthon
16,1-5	2265	194	Granite	Caledonian allochthon
16,1-12	1913	142	Granodiorite	Caledonian allochthon
16,1-15	1920	230	Granite/granodiorite	Caledonian allochthon
16,1-17	1988	82	Felsic, extremely weathered	Caledonian allochthon
16,1-18	2360	31	Granite	Caledonian allochthon
16,1-19	1891	104	Unknown	-
16,2-1	1873	33	Metamorphosed gneissic-granite	Caledonian allochthon
16,2-3	1894	9	Unknown	-
16,2-4	1879	121	Granodiorite	Caledonian allochthon
16,2-5	2342	31	Unknown	-
16,2-9	1986	96	Unknown	-
16,2-12	1939	128	Granite	Caledonian allochthon
16,2-17B	2133	67	Granite	Caledonian allochthon
16,2-18S	1864	106	Granite	Caledonian allochthon
16,2-19	1989	34	Granite	Caledonian allochthon
16,2-20	2183	32	Granite	Caledonian allochthon
16,3-2	2006	12	Monzogranite	Caledonian allochthon
16,3-4	1940	80	Monzogranite	Caledonian allochthon
16,3-6	1965	85	Granodiorite	Caledonian allochthon
16,3-7	2089	11	Granite	Caledonian allochthon
16,4-1	2885	44	Micaschist and granite	Caledonian allochthon
16,4-5	1898	122	Granodiorite	Caledonian allochthon
16,5-1	1925	20	Granodiorite, migmatite	Caledonian allochthon
16,6-1	2055	6	Dacite underlain by metamorphic schist	Caledonian allochthon
17,3-1	2811	41	Green schist	Caledonian allochthon
17,12-2	2300	34	Sandstone	Devonian
18,11-1	2060	26	Quartzite with chloritoschiste	Caledonian allochthon
25,6-1	2851	30	Metamorphosed granite and gneiss	Caledonian allochthon
25,7-1S	3551	41	Metasandstone and chlorite schist	Pre-Caledonian metasediment
25,10-2R	3152	29	Quartz-monzonite/schist anhydrite	Caledonian allochthon
25,11-1	2391	68	Gneissic schist overlaid by siltstone and sandstone	Caledonian allochthon/Devonian
25,11-17	2243	13	Phyllite	Basal décollement?
25,12-1	2425	440	Conglomerate and sandstone	Devonian
31,6-1	4014	56	Augengneiss overlaid by quartzitic sandstone	Pre-Caledonian metasediment
32,4-1	3132	54	Conglomerate (granitic) and Sandstone	Devonian?
35,3-2	4168	232	Green Mica schist/gneiss	Caledonian allochthon
35,3-4	4069	20	Green Mica schist/gneiss	Caledonian allochthon
35,3-5	4092	22	Green Mica schist/gneiss	Caledonian allochthon

35,9-1	2314	36	Green Mica schist/gneiss	Caledonian allochthon
35,9-2	2856	29	Green Mica schist/gneiss	Caledonian allochthon
35,9-3	2770	13	Metaquartzite, metamorphic	Pre-Caledonian metasediment
36,1-1	1568	27	Augengneiss	Proterozoic basement?
36,1-2	3233	22	Schist	Caledonian allochthon
36,4-1	2712	5	Greenschist	Caledonian allochthon
36,7-1	2834	7	Gneiss	Caledonian allochthon
36,7-2	1429	6	Greenschist	Caledonian allochthon
2-10a-10	1700	20	no data	-
2-10a-11	2225	22	no data	-
2-10a-12	2494	25	no data	-
2-10a-13	2562	18	no data	-
2-10a-6	1694	52	Schist and gneiss	Caledonian allochthon
2-10a-7Z	1809	35	Schist and gneiss	Caledonian allochthon
2-10a-8	2734	229	Mica schist and gneiss	Caledonian allochthon
2-10b-5	1343	25	Gneiss or sheared granite	Caledonian allochthon
2-10b-9	1331	31	Gneiss	Caledonian allochthon
2-15-1	1725	28	Schist and gneiss	Caledonian allochthon
2-15a-9	1628	17	Gneiss	Caledonian allochthon
2-20-1	1124	33	Gneiss	Caledonian allochthon
2-3-1	714	50	? Metamorphic	Caledonian allochthon
2-4-2	2335	19	Psammitic metamorphics (Metasandstone)	Devonian?
2-5-10	2610	41	Gneiss	Caledonian allochthon
2-5-11	2919	22	Gneiss	Caledonian allochthon
2-5-4	4131	13	Serpentinite	Caledonian allochthon
211-16-1	3330	21	Granite?	Caledonian allochthon
211-21-1A	3443	27	*Gneiss	Caledonian allochthon
211-21-2	3468	43	*Gneiss	Caledonian allochthon
211-26-1	3254	21	*Gneiss-Schist	Caledonian allochthon
211-26-2	3381	32	*Metasandstone	Devonian?
211-26-3	3509	72	*Metasandstone	Devonian?
3-11-1	2126	16	Granitic Gneiss	Caledonian allochthon
3-11-2	2520	19	Granite	Caledonian allochthon
3-11a-6	1981	33	Granite	Caledonian allochthon
3-11b-7	1891	29	*Granite	Caledonian allochthon
3-21-1	1989	18	Mica, gneiss and schist	Caledonian allochthon
3-3-4ARE	4407	36	*Gneiss	Caledonian allochthon

**Table S2** - Table showing basement penetrating exploration wells used in this study, after Fazlikhani et al. (2017). Depths shown are measured depth (MD) from the Kelly Bushing (KB) datum. Well information shown by asterisk is from Bassett (2003) and Marshall & Hewett (2003).